Table 3 Univariate and multivariate analyses of contributing factors associated with SVR

Parameter	Univariate analysis, OR (95% CI), P-value	Multivariate analysis, OR (95% CI), P-value
Age (years)	0.989 (0.968–1.011), 0.619	
Male/female	1.314 (0.886–1.949), 0.488	
Albumin (g/dL)	2.547 (1.399–4.637), 0.119	1.702 (0.728–3.979), 0.531
AST (U/L)	0.999 (0.995–1.005), 0.982	
ALT (U/L)	1.004 (1.001–1.007), 0.250	1.015 (1.009–1.020), 0.005
GGT (U/L)	0.989 (0.983–0.996), 0.101	0.981 (0.973–0.989), 0.022
Alkaline phosphatase (U/L)	0.995 (0.996–0.998), 0.101	0.998 (0.995–1.002), 0.698
Total bilirubin (mg/dL)	0.335 (0.166–0.679), 0.121	0.475 (0.257–0.877), 0.225
Prothrombin time activity (%)	1.002 (0.988–1.016), 0.895	
AFP (ng/mL)	0.984 (0.972–0.995), 0.154	0.999 (0.979–1.020), 0.986
Liver stiffness (kPa)	0.917 (0.884–0.952), 0.019	0.866 (0.810–0.927), 0.033
Platelet (×10⁴/μL)	1.030 (0.997–1.065), 0.366	0.958 (0.913–1.006), 0.381
HCV RNA viral load (KIU/mL)	0.850 (0.561–1.287), 0.695	
PLNE	0.318 (0.176–0.576), 0.053	0.179 (0.090–0.354), 0.012

AFP, α-fetoprotein; ALT, alanine aminotransferase; AST, aspartate aminotransferase; CI, confidence interval; GGT, γ-glutamyltransferase; HCV, hepatitis C virus; IL, interleukin; OR, odds ratio; PLNE, perihepatic lymph node enlargement; SVR, sustained virological response.

Association between PLNE and the mutations at position 70 of HCV core protein and at ISDR or IL-28B polymorphism

Recently, as a human factor, *IL-28B* polymorphism has been shown to be a strong predictor for the response to PEG IFN and RBV therapy for chronic hepatitis C.[21–23] On the other hand, as a viral factor, the mutations at position 70 of HCV core protein[24] and those at ISDR of NS5A protein[25] have been revealed to be associated with the treatment outcome by IFN. Thus, the potential associations between PLNE and these factors were evaluated. To this end, we first sought to analyze them in the original cohort, however, the stored samples were not enough for these determinations. Thus, we newly enrolled 45 chronic hepatitis C patients to only assess the potential associations between PLNE and *IL-28B* polymorphism, the mutations at position 70 of HCV core protein or those at ISDR of NS5A protein.

The clinical features of these 45 patients with chronic hepatitis C with HCV genotype 1 are summarized in Table 4. Among these patients, PLNE was observed in 18 patients (40%). Regarding *IL-28B* genotypes, the frequency of the rs8099917 risk allele (G), namely, minor allele, was not different between the patients with PLNE and those without: 22.2% in the former and 23.1% in the latter ($P = 0.76$ by χ^2-test; Fig. 2a). As a viral factor, the mutations at position 70 of HCV core protein were observed in 44.4% patients with PLNE, and in 42.3% patients without ($P = 0.87$ by χ^2-test; Fig. 2b), and less

than two substitutions at ISDR were observed in 52.9% patients with PLNE, and in 64.0% patients without ($P = 0.69$ by χ^2-test; Fig. 2c), none of which were statistically different. These results suggest that PLNE is not associated with *IL-28B* polymorphism, or the mutations

Table 4 Characteristics of patients in whom the mutations at position 70 of HCV core protein and at ISDR or IL-28B polymorphism were measured

Parameter	n = 45
Age (years)†	68.1 ± 10.7
Male/female	19/26
Albumin (g/dL)†	3.93 ± 0.39
AST (U/L)†	43.4 ± 18.6
ALT (U/L)†	38.8 ± 20.3
GGT (U/L)†	38.1 ± 28.9
Alkaline phosphatase (U/L)†	276.3 ± 101.5
Total bilirubin (mg/dL)†	0.83 ± 0.29
Prothrombin time activity (%)	99.1 ± 2.86
AFP (ng/mL)†	16.0 ± 36.3
Platelet count (×10⁴/μL)†	15.4 ± 7.0
HCV viral load (log IU/mL)‡	5.94 (5.54–6.60)
PLNE positive/negative	18/27

†Data are presented as mean ± standard deviation.
‡Data are presented as median (25–75% range).
AFP, α-fetoprotein; ALT, alanine aminotransferase; AST, aspartate aminotransferase; GGT, γ-glutamyltransferase; HCV, hepatitis C virus; IL, interleukin; ISDR, interferon sensitivity-determining region; PLNE, perihepatic lymph node enlargement;.
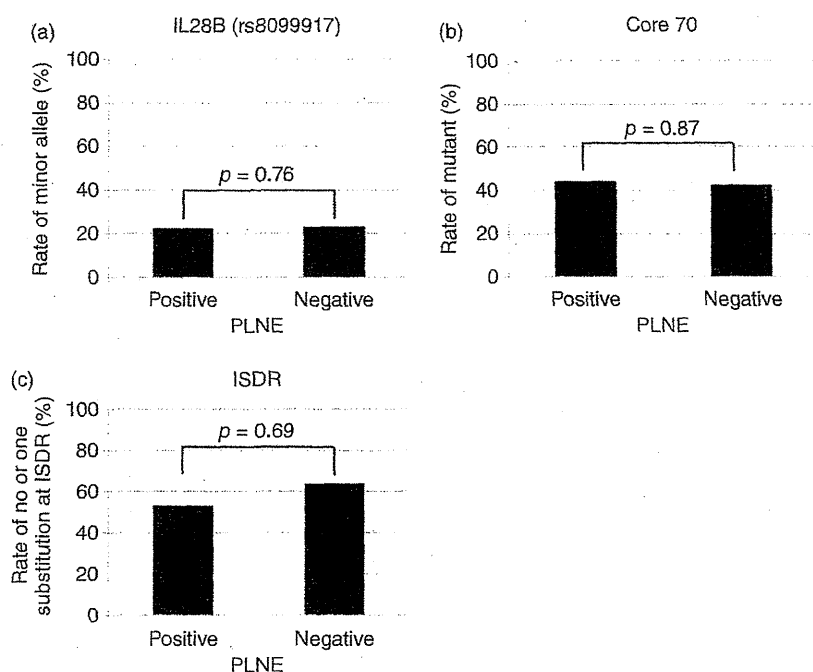
Figure 2 Rate of IL-28B minor allele (a), mutant at position 70 of HCV core protein (Core 70, b), and no or one substitution at ISDR (c) in patients with PLNE (positive) or without PLNE (negative). The rate of IL-28B minor allele (a), mutant at position 70 of HCV core protein (Core 70, b), and no or one substitutions at ISDR (c) was analyzed in patients with PLNE (positive, $n = 18$) or without PLNE (negative, $n = 27$). HCV, hepatitis C virus; IL, interleukin; ISDR, interferon sensitivity-determining region; PLNE, perihepatic lymph node enlargement.

at position 70 of HCV core protein and those at ISDR of NS5A protein.

DISCUSSION

THE FACT THAT chronic hepatitis C patients with PLNE are prone to treatment failure to IFN therapy has been previously reported.[10-12] However, there were limitations because these analyses were performed in patients with various HCV genotypes, viral loads and treatment regimens. It is well known that efficacy of IFN therapy for chronic hepatitis C is poorest in patients with HCV genotype 1 and higher HCV viral load.[13] On the other hand, IFN therapy has been refined with PEG and combination with RBV and protease inhibitors.[26] Thus, to more precisely examine the potential association between PLNE and efficacy of IFN therapy for chronic hepatitis C patients, we sought to analyze the efficacy of PEG IFN and RBV therapy on patients with HCV genotype 1 and HCV RNA of more than 100 KIU/mL in the presence or absence of PLNE. As a result, the SVR rate was significantly lower and the viral decline during the first 4 weeks of treatment was significantly smaller in patients with PLNE than in those without, and PLNE was negatively associated with SVR by multivariate analysis. It is noteworthy that PLNE was not associated with liver stiffness values, a marker

of liver fibrosis,[27] although controversy exists whether PLNE may be associated with liver fibrosis,[2,4] and more importantly that PLNE was retained as a negative predictor for SVR by multivariate analysis, independent of liver fibrosis, in the current study.

To examine the underlying mechanism in the association between PLNE and efficacy of PEG IFN and RBV for chronic hepatitis C, we analyzed the potential links between PLNE and well-established host or viral factors to predict outcome by IFN therapy. We especially considered the possibility that PLNE may be associated with *IL-28B* polymorphism, which could be importantly involved in the host immune system.[21-23] However, PLNE was not significantly associated with *IL-28B* polymorphism as a host factor, in addition to no association of PLNE with the mutations at position 70 of HCV core protein[24] and those at ISDR[25] as a viral factor. Thus, we speculate that PLNE may reflect an unknown host factor to play a role in the reaction to HCV infection.

Perihepatic lymph node enlargement in chronic hepatitis C has long been assumed to reflect the immunological response of the host.[7] Indeed, higher CD8+ lymphocyte levels in the blood were observed in chronic hepatitis C patients with PLNE,[7] and HCV-specific IFN-γ production and proliferative response of T cells were found commonly in perihepatic lymph node,[28] suggesting that PLNE indicates an active host immune response

in chronic hepatitis C. Of interest is the finding that biochemical responders to IFN-α therapy for chronic hepatitis C had significantly lower pretreatment levels of CD8^{+} cells.[29] Thus, increased CD8^{+} cell levels in chronic hepatitis C patients with PLNE[7] may explain the mechanism, at least in part, of the association between PLNE and the poorer outcome by PEG IFN and RBV therapy. Furthermore, increased oligoclonality of circulating CD8^{+} cells in chronic HCV infection was also identified as an indicator for poor clinical response to IFN-α therapy.[30] It should be further clarified whether the altered clonality of CD8^{+} cells may be also involved in the mechanism of the association between PLNE and the efficacy of PEG IFN and RBV therapy.

We previously demonstrated that PLNE is a negative risk for hepatocarcinogenesis in chronic hepatitis C.[10] Currently, we have found that PLNE is a negative predictor for a successful outcome of IFN treatment for chronic hepatitis C, both of which could be paradoxical. However, these findings may be consistently explained by an active host immune system as described above. We previously speculated that the reduced hepatocarcinogenesis in chronic hepatitis C patients with PLNE may be explained by the enhanced host immune system. On the other hand, there are accumulating lines of evidence suggesting that the originally enhanced host immune response may be associated with a negative outcome of IFN treatment for chronic hepatitis C; the higher expression of IFN-stimulated genes in the liver was observed in patients with no response to IFN treatment for chronic hepatitis C.[31–35] Thus, we speculate that PLNE, as an indicator of active host immune responses,[7,28] may be associated negatively with the efficacy of IFN therapy for chronic hepatitis C in line with these previous studies.

One of the limitations of the current study is that the association between PLNE and efficacy of IFN therapy in chronic hepatitis C patients was determined in the retrospective cohort. However, the cohort analyzed was originally set up to prospectively examine the risk of liver stiffness values for HCC development, where patients were consecutively enrolled among those who previously visited our Department of Gastroenterology, The University of Tokyo Hospital,[15] and were followed up for 4.8 years.[10] Thus, we believe that our current evidence could be the same as that from the prospective cohort. As another limitation, the association between PLNE and *IL-28B* polymorphism, the mutations at position 70 of HCV core protein or those at ISDR could not be assessed in the original cohort, because the stored samples of the original cohort were not enough for these determinations.

The combination of PEG IFN and RBV has been the standard of care for chronic hepatitis C,[26] and the further combination of telaprevir[36] or boceprevir[37] with PEG IFN and RBV has been recently employed to improve the treatment efficacy. Nonetheless, it is expected that IFN is still going to play a role in the treatment for chronic hepatitis C. Thus, our evidence of PLNE as a significant predictor for SVR by PEG IFN and RBV therapy may be useful when deciding upon the regimen or timing treatment for chronic hepatitis C patients. Furthermore, because PLNE is originally one of the common clinical signs of chronic liver disease,[1–3] the knowledge regarding the clinical significance of PLNE may shed a light on not only the prediction of treatment outcome of IFN therapy for chronic hepatitis C but also the general pathophysiology of chronic liver disease.

REFERENCES

1 Cassani F, Zoli M, Baffoni L *et al.* Prevalence and significance of abdominal lymphadenopathy in patients with chronic liver disease: an ultrasound study. *J Clin Gastroenterol* 1990; 12: 42–6.

2 Cassani F, Valentini P, Cataleta M *et al.* Ultrasound-detected abdominal lymphadenopathy in chronic hepatitis C: high frequency and relationship with viremia. *J Hepatol* 1997; 26: 479–83.

3 Dietrich CF, Lee JH, Herrmann G *et al.* Enlargement of perihepatic lymph nodes in relation to liver histology and viremia in patients with chronic hepatitis C. *Hepatology* 1997; 26: 467–72.

4 Soresi M, Carroccio A, Agate V *et al.* Evaluation by ultrasound of abdominal lymphadenopathy in chronic hepatitis C. *Am J Gastroenterol* 1999; 94: 497–501.

5 Zhang XM, Mitchell DG, Shi H *et al.* Chronic hepatitis C activity: correlation with lymphadenopathy on MR imaging. *AJR Am J Roentgenol* 2002; 179: 417–22.

6 del Olmo JA, Esteban JM, Maldonado L *et al.* Clinical significance of abdominal lymphadenopathy in chronic liver disease. *Ultrasound Med Biol* 2002; 28: 297–301.

7 Muller P, Renou C, Harafa A *et al.* Lymph node enlargement within the hepatoduodenal ligament in patients with chronic hepatitis C reflects the immunological cellular response of the host. *J Hepatol* 2003; 39: 807–13.

8 Watanabe T, Sassa T, Hiratsuka H, Hattori S, Abe A. Clinical significance of enlarged perihepatic lymph node on ultrasonography. *Eur J Gastroenterol Hepatol* 2005; 17: 185–90.

9 Tavakoli-Tabasi S, Ninan S. Clinical significance of perihepatic lymphadenopathy in patients with chronic hepatitis C infection. *Dig Dis Sci* 2011; 56: 2137–44.

10 Hikita H, Nakagawa H, Tateishi R *et al.* Perihepatic lymph node enlargement is a negative predictor of liver cancer

development in chronic hepatitis C patients. *J Gastroenterol.* Epub ahead of print: DOI 10.1007/s00535-012-0635-7.

11 Dietrich CF, Stryjek-Kaminska D, Teuber G, Lee JH, Caspary WF, Zeuzem S. Perihepatic lymph nodes as a marker of antiviral response in patients with chronic hepatitis C infection. *AJR Am J Roentgenol* 2000; 174: 699–704.

12 Soresi M, Bonfissuto G, Sesti R *et al.* Perihepatic lymph nodes and antiviral response in chronic HCV-associated hepatitis. *Ultrasound Med Biol* 2004; 30: 711–17.

13 Shiratori Y, Kato N, Yokosuka O *et al.* Predictors of the efficacy of interferon therapy in chronic hepatitis C virus infection. Tokyo-Chiba Hepatitis Research Group. *Gastroenterology* 1997; 113: 558–66.

14 Manns MP, McHutchison JG, Gordon SC *et al.* Peginterferon alfa-2b plus ribavirin compared with interferon alfa-2b plus ribavirin for initial treatment of chronic hepatitis C: a randomised trial. *Lancet* 2001; 358: 958–65.

15 Masuzaki R, Tateishi R, Yoshida H *et al.* Prospective risk assessment for hepatocellular carcinoma development in patients with chronic hepatitis C by transient elastography. *Hepatology* 2009; 49: 1954–61.

16 Ibarrola N, Moreno-Monteagudo JA, Saiz M *et al.* Response to retreatment with interferon-alpha plus ribavirin in chronic hepatitis C patients is independent of the NS5A gene nucleotide sequence. *Am J Gastroenterol* 1999; 94: 2487–95.

17 Hayashi K, Katano Y, Ishigami M *et al.* Mutations in the core and NS5A region of hepatitis C virus genotype 1b and correlation with response to pegylated-interferon-alpha 2b and ribavirin combination therapy. *J Viral Hepat* 2011; 18: 280–6.

18 Akkarathamrongsin S, Sugiyama M, Matsuura K *et al.* High sensitivity assay using serum sample for IL28B genotyping to predict treatment response in chronic hepatitis C patients. *Hepatol Res* 2010; 40: 956–62.

19 Gargiulo F, De Francesco MA, Pinsi G *et al.* Determination of HCV genotype by direct sequence analysis of quantitative PCR products. *J Med Virol* 2003; 69: 202–6.

20 Tsubota A, Chayama K, Ikeda K *et al.* Factors predictive of response to interferon-alpha therapy in hepatitis C virus infection. *Hepatology* 1994; 19: 1088–94.

21 Ge D, Fellay J, Thompson AJ *et al.* Genetic variation in IL28B predicts hepatitis C treatment-induced viral clearance. *Nature* 2009; 461: 399–401.

22 Tanaka Y, Nishida N, Sugiyama M *et al.* Genome-wide association of IL28B with response to pegylated interferon-alpha and ribavirin therapy for chronic hepatitis C. *Nat Genet* 2009; 41: 1105–9.

23 Suppiah V, Moldovan M, Ahlenstiel G *et al.* IL28B is associated with response to chronic hepatitis C interferon-alpha and ribavirin therapy. *Nat Genet* 2009; 41: 1100–4.

24 Akuta N, Suzuki F, Sezaki H *et al.* Association of amino acid substitution pattern in core protein of hepatitis C virus

genotype 1b high viral load and non-virological response to interferon-ribavirin combination therapy. *Intervirology* 2005; 48: 372–80.

25 Enomoto N, Sakuma I, Asahina Y *et al.* Comparison of full-length sequences of interferon-sensitive and resistant hepatitis C virus 1b. Sensitivity to interferon is conferred by amino acid substitutions in the NS5A region. *J Clin Invest* 1995; 96: 224–30.

26 Afdhal NH, McHutchison JG, Zeuzem S *et al.* Hepatitis C pharmacogenetics: state of the art in 2010. *Hepatology* 2011; 53: 336–45.

27 Castera L, Vergniol J, Foucher J *et al.* Prospective comparison of transient elastography, Fibrotest, APRI, and liver biopsy for the assessment of fibrosis in chronic hepatitis C. *Gastroenterology* 2005; 128: 343–50.

28 Moonka D, Milkovich KA, Rodriguez B, Abouljoud M, Lederman MM, Anthony DD. Hepatitis C virus-specific T-cell gamma interferon and proliferative responses are more common in perihepatic lymph nodes than in peripheral blood or liver. *J Virol* 2008; 82: 11742–8.

29 Saito H, Ebinuma H, Satoh I *et al.* Immunological and virological predictors of outcome during interferon-alpha therapy of chronic hepatitis C. *J Viral Hepat* 2000; 7: 64–74.

30 Manfras BJ, Weidenbach H, Beckh KH *et al.* Oligoclonal CD8+ T-cell expansion in patients with chronic hepatitis C is associated with liver pathology and poor response to interferon-alpha therapy. *J Clin Immunol* 2004; 24: 258–71.

31 Chen L, Borozan I, Feld J *et al.* Hepatic gene expression discriminates responders and nonresponders in treatment of chronic hepatitis C viral infection. *Gastroenterology* 2005; 128: 1437–44.

32 Feld JJ, Nanda S, Huang Y *et al.* Hepatic gene expression during treatment with peginterferon and ribavirin: identifying molecular pathways for treatment response. *Hepatology* 2007; 46: 1548–63.

33 Sarasin-Filipowicz M, Oakeley EJ, Duong FH *et al.* Interferon signaling and treatment outcome in chronic hepatitis C. *Proc Natl Acad Sci U S A* 2008; 105: 7034–9.

34 Asselah T, Bieche I, Narguet S *et al.* Liver gene expression signature to predict response to pegylated interferon plus ribavirin combination therapy in patients with chronic hepatitis C. *Gut* 2008; 57: 516–24.

35 Honda M, Sakai A, Yamashita T *et al.* Hepatic ISG expression is associated with genetic variation in interleukin 28B and the outcome of IFN therapy for chronic hepatitis C. *Gastroenterology* 2010; 139: 499–509.

36 Jacobson IM, McHutchison JG, Dusheiko G *et al.* Telaprevir for previously untreated chronic hepatitis C virus infection. *N Engl J Med* 2011; 364: 2405–16.

37 Poordad F, McCone J, Jr, Bacon BR *et al.* Boceprevir for untreated chronic HCV genotype 1 infection. *N Engl J Med* 2011; 364: 1195–206.

Cell

Identification of Liver Cancer Progenitors Whose Malignant Progression Depends on Autocrine IL-6 Signaling

Guobin He,[1,13] Debanjan Dhar,[1,13] Hayato Nakagawa,[1,11,13] Joan Font-Burgada,[1,13] Hisanobu Ogata,[1,12,13] Yuhong Jiang,[1] Shabnam Shalapour,[1] Ekihiro Seki,[2] Shawn E. Yost,[4,5] Kristen Jepsen,[5] Kelly A. Frazer,[5,6,7,8] Olivier Harismendy,[5,6,7] Maria Hatziapostolou,[9] Dimitrios Iliopoulos,[9] Atsushi Suetsugu,[3,10] Robert M. Hoffman,[3,10] Ryosuke Tateishi,[11] Kazuhiko Koike,[11] and Michael Karin[1,6,*]

[1]Laboratory of Gene Regulation and Signal Transduction, Departments of Pharmacology and Pathology
[2]Department of Medicine
[3]Department of Surgery
[4]Bioinformatics Graduate Program
[5]Rady's Children's Hospital and Department of Pediatrics
[6]Moores UCSD Cancer Center
[7]Clinical and Translational Research Institute
[8]Institute for Genomic Medicine
University of California San Diego, School of Medicine, 9500 Gilman Drive, San Diego, CA 92093, USA
[9]Center for Systems Biomedicine, Division of Digestive Diseases and Institute for Molecular Medicine, David Geffen School of Medicine, University of California Los Angeles, Los Angeles, CA 90095, USA
[10]AntiCancer, Inc., San Diego, CA 92111, USA
[11]Department of Gastroenterology, University of Tokyo, Tokyo 113-8655, Japan
[12]Department of Medicine and Clinical Science, Graduate School of Medical Sciences, Kyushu University, Fukuoka 812-8582, Japan
[13]These authors contributed equally to this work
*Correspondence: karinoffice@ucsd.edu
http://dx.doi.org/10.1016/j.cell.2013.09.031

SUMMARY

Hepatocellular carcinoma (HCC) is a slowly developing malignancy postulated to evolve from premalignant lesions in chronically damaged livers. However, it was never established that premalignant lesions actually contain tumor progenitors that give rise to cancer. Here, we describe isolation and characterization of HCC progenitor cells (HcPCs) from different mouse HCC models. Unlike fully malignant HCC, HcPCs give rise to cancer only when introduced into a liver undergoing chronic damage and compensatory proliferation. Although HcPCs exhibit a similar transcriptomic profile to bipotential hepatobiliary progenitors, the latter do not give rise to tumors. Cells resembling HcPCs reside within dysplastic lesions that appear several months before HCC nodules. Unlike early hepatocarcinogenesis, which depends on paracrine IL-6 production by inflammatory cells, due to upregulation of LIN28 expression, HcPCs had acquired autocrine IL-6 signaling that stimulates their in vivo growth and malignant progression. This may be a general mechanism that drives other IL-6-producing malignancies.

INTRODUCTION

Every malignant tumor is probably derived from a single progenitor that had acquired growth and survival advantages through genetic and epigenetic changes, allowing clonal expansion (Nowell, 1976). Tumor progenitors are not necessarily identical to cancer stem cells (CSCs), which maintain and renew fully established malignancies (Nguyen et al., 2012). However, clonal evolution and selective pressure may cause some descendants of the initial progenitor to cross the bridge of no return and form a premalignant lesion. Cancer genome sequencing indicates that most cancers require at least five genetic changes to evolve (Wood et al., 2007). How these changes affect the properties of tumor progenitors and control their evolution into a CSC is not entirely clear, as it has been difficult to isolate and propagate cancer progenitors prior to detection of tumor masses. Given these difficulties, it is also not clear whether cancer progenitors are the precursors for the more malignant CSC isolated from fully established cancers. An answer to these critical questions depends on identification and isolation of cancer progenitors, which may also enable definition of molecular markers and signaling pathways suitable for early detection and treatment. This is especially important in cancers of the liver and pancreas, which evolve over the course of many years but, once detected, are extremely difficult to treat (El-Serag, 2011; Hruban et al., 2007).

Hepatocellular carcinoma (HCC), the most common liver cancer, is the end product of chronic liver diseases, requiring

CrossMark

several decades to evolve (El-Serag, 2011). Currently, HCC is the third most deadly and fifth most common cancer worldwide, and in the United States its incidence has doubled in the past two decades. Furthermore, 8% of the world's population are chronically infected with hepatitis B or C viruses (HBV and HCV) and are at a high risk of new HCC development (El-Serag, 2011). Up to 5% of HCV patients will develop HCC in their lifetime, and the yearly HCC incidence in patients with cirrhosis is 3%–5%. These tumors may arise from premalignant lesions, ranging from dysplastic foci to dysplastic hepatocyte nodules that are often seen in damaged and cirrhotic livers and are more proliferative than the surrounding parenchyma (Hytiroglou et al., 2007). However, the tumorigenic potential of these lesions was never examined, and it is unknown whether they contain any genetic alterations. Given that there is no effective treatment for HCC and, upon diagnosis, most patients with advanced disease have a remaining lifespan of 4–6 months, it is important to detect HCC early, while it is still amenable to surgical resection or chemotherapy. Premalignant lesions, called foci of altered hepatocytes (FAH), were also described in chemically induced HCC models (Pitot, 1990), but it was questioned whether these lesions harbor tumor progenitors or result from compensatory proliferation (Sell and Leffert, 2008). The aim of this study was to determine whether HCC progenitor cells (HcPCs) exist and if so, to isolate these cells and identify some of the signaling networks that are involved in their maintenance and progression.

We now describe HcPC isolation from mice treated with the procarcinogen diethyl nitrosamine (DEN), which induces poorly differentiated HCC nodules within 8 to 9 months (Verna et al., 1996). Although these tumors do not evolve in the context of cirrhosis, the use of a chemical carcinogen is justified because the finding of up to 121 mutations per HCC genome suggests that carcinogens may be responsible for human HCC induction (Guichard et al., 2012). Furthermore, 20%–30% of HCC, especially in HBV-infected individuals, evolve in noncirrhotic livers (El-Serag, 2011). Nonetheless, we also isolated HcPCs from $Tak1^{\Delta hep}$ mice, which develop spontaneous HCC as a result of progressive liver damage, inflammation, and fibrosis caused by ablation of TAK1 (Inokuchi et al., 2010). Although the etiology of each model is distinct, both contain HcPCs that express marker genes and signaling pathways previously identified in human HCC stem cells (Marquardt and Thorgeirsson, 2010) long before visible tumors are detected. Furthermore, DEN-induced premalignant lesions and HcPCs exhibit autocrine IL-6 production that is critical for tumorigenic progression. Circulating IL-6 is a risk indicator in several human pathologies and is strongly correlated with adverse prognosis in HCC and cholangiocarcinoma (Porta et al., 2008; Soresi et al., 2006). IL-6 produced by in-vitro-induced CSCs was suggested to be important for their maintenance (Iliopoulos et al., 2009). Furthermore, autocrine IL-6 was detected in several cancers, but its origin is poorly understood (Grivennikov and Karin, 2008). In particular, little is known about the source of IL-6 in HCC. In early stages of hepatocarcinogenesis, IL-6 is produced by Kupffer cells or macrophages (Maeda et al., 2005; Naugler et al., 2007). However, paracrine IL-6 production is transient and does not explain its expression by HCC cells.

RESULTS

DEN-Induced Collagenase-Resistant Aggregates of HCC Progenitors

A single intraperitoneal (i.p.) injection of DEN into 15-day-old BL/6 mice induces HCC nodules first detected 8 to 9 months later. However, hepatocytes prepared from macroscopically normal livers 3 months after DEN administration already contain cells that progress to HCC when transplanted into the permissive liver environment of MUP-uPA mice (He et al., 2010), which express urokinase plasminogen activator (uPA) from a mouse liver-specific major urinary protein (MUP) promoter and undergo chronic liver damage and compensatory proliferation (Rhim et al., 1994). Collagenase digestion of DEN-treated livers generated a mixture of monodisperse hepatocytes and aggregates of tightly packed small hepatocytic cells (Figure 1A). Aggregated cells were also present—but in lower abundance—in digests of control livers (Figure S1A available online). HCC markers such as α fetoprotein (AFP), glypican 3 (Gpc3), and Ly6D, whose expression in mouse liver cancer was reported (Meyer et al., 2003), were upregulated in aggregates from DEN-treated livers, but not in nonaggregated hepatocytes or aggregates from control livers (Figure S1A). Thus, control liver aggregates may result from incomplete collagenase digestion, whereas aggregates from DEN-treated livers may contain HcPC. DEN-induced aggregates became larger and more abundant 5 months after carcinogen exposure, when they consisted of 10–50 cells that were smaller than nonaggregated hepatocytes. Using 70 μm and 40 μm sieves, we separated aggregated from nonaggregated hepatocytes (Figure 1A) and tested their tumorigenic potential by transplantation into MUP-uPA mice (Figure 1B). To facilitate transplantation, the aggregates were mechanically dispersed and suspended in Dulbecco's modified Eagle's medium (DMEM). Five months after intrasplenic (i.s.) injection of 10^4 viable cells, mice receiving cells from aggregates developed about 18 liver tumors per mouse, whereas mice receiving nonaggregated hepatocytes developed less than 1 tumor each (Figure 1B). The tumors exhibited typical trabecular HCC morphology and contained cells that abundantly express AFP (Figure S1B). To confirm that the HCCs were derived from transplanted cells, we measured their relative MUP-uPA DNA copy number and found that they contained much less MUP-uPA transgene DNA than the surrounding parenchyma (Figure S1C). Transplantation of aggregated cells from livers of DEN-treated actin-GFP transgenic mice resulted in GFP-positive HCCs (Figure S1D). Both experiments strongly suggest that the HCCs were derived from the transplanted cells. No tumors were ever observed after transplantation of control hepatocytes (nonaggregated or aggregated).

Only liver tumors were formed by the transplanted cells. Other organs, including the spleen into which the cells were injected, remained tumor free (Figure 1B), suggesting that HcPCs progress to cancer only in the proper microenvironment. Indeed, no tumors appeared after HcPC transplantation into normal BL/6 mice. But, if BL/6 mice were first treated with retrorsine (a chemical that permanently inhibits hepatocyte proliferation [Laconi et al., 1998]), intrasplenically transplanted with HcPC-containing aggregates, and challenged with CCl_4 to induce liver injury and compensatory proliferation (Guo et al., 2002), HCCs readily
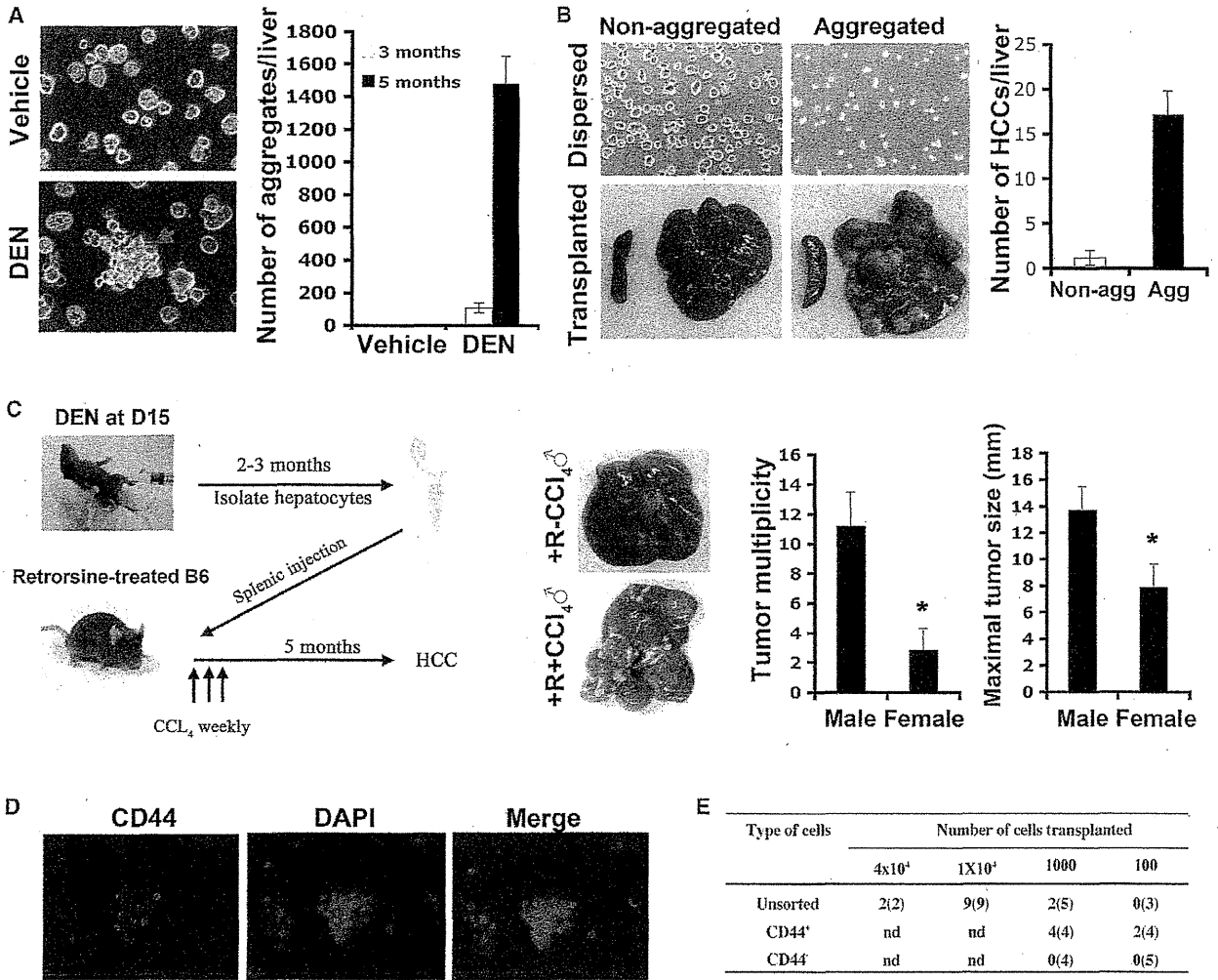
Figure 1. DEN-Induced Hepatocytic Aggregates Contain CD44+ HCC Progenitors

(A) Fifteen-day-old BL/6 males were given DEN or vehicle. After 3 or 5 months, their livers were removed and collagenase digested. Left: typical digest appearance (magnification: 400×; 3 months after DEN). Red arrow indicates a collagenase-resistant aggregate. Right: aggregates per liver (n = 5; ± SD for each point).

(B) Livers were collagenase digested 5 months after DEN administration. Aggregates were separated from nonaggregated cells and mechanically dispersed into a single-cell suspension (left upper panels; 200×). 10^4 viable aggregated or nonaggregated cells were i.s. injected into MUP-uPA mice whose livers and spleens were analyzed for tumors 5 months later (left lower panels). The number of HCC nodules per liver was determined (n = 5; ± SD).

(C) Adult BL/6 mice were given retrorsine twice with a 2 week interval to inhibit hepatocyte proliferation. After 1 month, mice were i.s. transplanted with dispersed hepatocyte aggregates (10^4 cells) from DEN-treated mice and, 2 weeks later, were given three weekly i.p. injections of CCl_4 or vehicle. Tumor multiplicity and size were evaluated 5 months later (n = 5; ± SD).

(D) Hepatocyte aggregates were prepared as in (A), stained with CD44 antibody and DAPI, and examined by fluorescent microscopy (400×).

(E) Hepatocyte aggregates were dispersed as above, and CD44+ cells were separated from CD44− cells. The indicated cell numbers were injected into MUP-uPA mice, and HCC development was evaluated 5 months later. n values are in parentheses (n.d., not done).

See also Figure S1.

appeared (Figure 1C). CCl_4 omission prevented tumor development. Notably, MUP-uPA or CCl_4-treated livers are fragile, rendering direct intrahepatic transplantation difficult. The transplanted HcPC-containing aggregates formed more numerous and larger HCC nodules in male recipients than in females (Figure 1C), as observed in MUP-uPA mice transplanted with unfractionated DEN-exposed hepatocytes (He et al., 2010). Thus,

CCl_4-induced liver damage, especially within a male liver, generates a microenvironment that drives HcPC proliferation and malignant progression. To examine this point, we transplanted GFP-labeled HcPC-containing aggregates into retrorsine-treated BL/6 mice and examined their ability to proliferate with or without subsequent CCl_4 treatment. Indeed, the GFP+ cells formed clusters that grew in size only in CCl_4-treated host livers
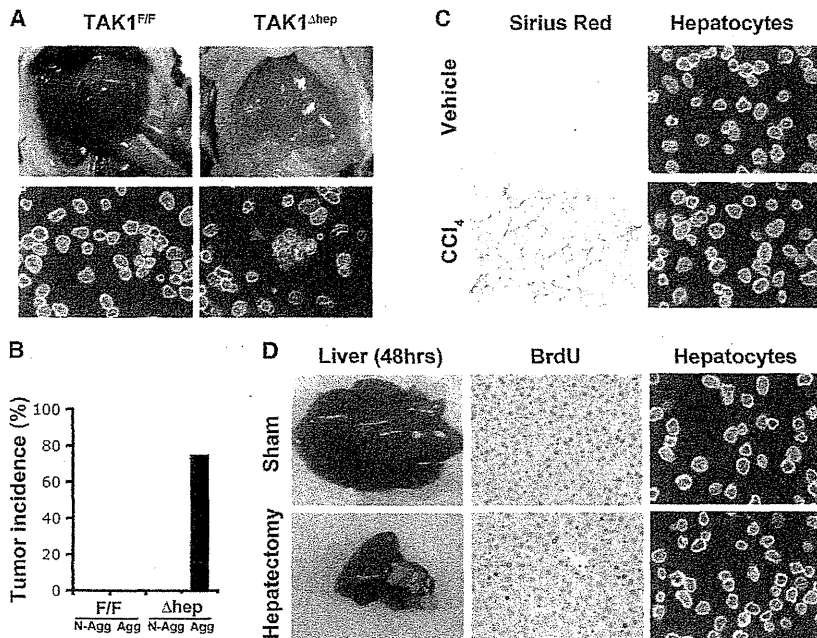
Figure 2. Tak1$^{\Delta hep}$ Livers Contain Collagenase-Resistant HcPC Aggregates

(A) Livers, free of tumors (upper panels), were removed from 1-month-old Tak1$^{F/F}$ and Tak1$^{\Delta hep}$ males and collagenase digested (lower panels; red arrow indicates collagenase-resistant aggregate).

(B) 10^4 nonaggregated or dispersed aggregated hepatocytes from (A) were i.s. injected into MUP-uPA mice that were analyzed 6 months later to identify mice with at least one liver tumor (n = 5–8 mice per genotype).

(C) BL/6 males were injected with vehicle or CCl$_4$ twice weekly for 2 weeks. Hepatocytes were isolated by collagenase digestion and photographed (right panels; 400×). Liver sections were stained with Sirius red to reveal collagen deposits (left panels).

(D) 8-week-old BL/6 males were subjected to 70% partial hepatectomy, pulsed with BrdU at 46 and 70 hr, and sacrificed 2 hr later. Isolated hepatocytes were photographed. Liver sections were analyzed for BrdU incorporation (400×). See also Figure S2 and Table S1.

(Figure S1E). Omission of CCl$_4$ prevented their expansion. Unlike HCC-derived cancer cells (dih10 cells), which form subcutaneous (s.c.) tumors with HCC morphology (He et al., 2010; Park et al., 2010), the HcPC-containing aggregates did not generate s.c. tumors in BL/6 mice (Figure S1F).

Despite their homogeneous appearance, the HcPC-containing aggregates contained both CD44$^+$ and CD44$^-$ cells (Figure 1D). Because CD44 is expressed by HCC stem cells (Yang et al., 2008; Zhu et al., 2010), we dispersed the aggregates and separated CD44$^+$ from CD44$^-$ cells and transplanted both into MUP-uPA mice. Whereas as few as 10^3 CD44$^+$ cells gave rise to HCCs in 100% of recipients, no tumors were detected after transplantation of CD44$^-$ cells (Figure 1E). Remarkably, 50% of recipients developed at least one HCC after receiving as few as 10^2 CD44$^+$ cells. Mature CD44$^-$ hepatocytes were found to engraft as well as or better than CD44$^+$ small hepatocytic cells (Haridass et al., 2009; Ichinohe et al., 2012). Hence, livers of DEN-treated mice contain CD44$^+$ HcPC that can be successfully isolated and purified and give rise to HCCs after transplantation into appropriate hosts. Unlike fully transformed HCC cells, HcPCs only give rise to tumors within the liver.

HcPC-Containing Aggregates in Tak1$^{\Delta hep}$ Mice

We applied the same HcPC isolation protocol to Tak1$^{\Delta hep}$ mice, which develop HCC of different etiology from DEN-induced HCC. Importantly, Tak1$^{\Delta hep}$ mice develop HCC as a consequence of chronic liver injury and fibrosis without carcinogen or toxicant exposure (Inokuchi et al., 2010). Indeed, whole-tumor exome sequencing revealed that DEN-induced HCC contained about 24 mutations per 10^6 bases (Mb) sequenced, with B-Raf^{V637E} being the most recurrent, whereas 1.4 mutations per Mb were detected in Tak1$^{\Delta hep}$ HCC's exome (Table S1). By contrast, Tak1$^{\Delta hep}$ HCC exhibited gene copy number changes.

Collagenase digests of 1-month-old Tak1$^{\Delta hep}$ livers contained much more hepatocytic aggregates than Tak1$^{f/f}$ liver digests (Figure 2A). Notably, HCC developed in 75% of MUP-uPA mice that received dispersed Tak1$^{\Delta hep}$ aggregates, but no tumors appeared in mice receiving nonaggregated Tak1$^{\Delta hep}$ or total Tak1$^{f/f}$ hepatocytes (Figure 2B). Because Tak1$^{\Delta hep}$ mice are subject to chronic liver damage and consequent compensatory proliferation, we wanted to ascertain that the HcPCs are not simply proliferating hepatocytes or expanding bipotential hepatobiliary progenitors using CCl$_4$ to induce liver injury and compensatory proliferation in WT mice. Although this treatment caused acute liver fibrosis, it did not augment formation of collagenase-resistant aggregates (Figure 2C). Similarly, few aggregates were detected in collagenase digests of livers after partial hepatectomy (Figure 2D). However, bile duct ligation (BDL) or feeding with 3,5-dicarbethoxy-1,4-dihydrocollidine (DDC), treatments that cause cholestatic liver injuries and oval cell expansion (Dorrell et al., 2011), did increase the number of small hepatocytic cell aggregates (Figure S2A). Nonetheless, no tumors were observed 5 months after injection of such aggregates into MUP-uPA mice (Figure S2B). Thus, not all hepatocytic aggregates contain HcPCs, and HcPCs only appear under tumorigenic conditions.

The HcPC Transcriptome Is Similar to that of HCC and Oval Cells

To determine the relationship between DEN-induced HcPCs, normal hepatocytes, and fully transformed HCC cells, we analyzed the transcriptomes of aggregated and nonaggregated hepatocytes from male littermates 5 months after DEN administration, HCC epithelial cells from DEN-induced tumors, and normal hepatocytes from age- and gender-matched littermate controls. Clustering analysis distinguished the HCC samples from other samples and revealed that the aggregated

A

HCC vs Aggregated Cells

log2(Tumor/Norm) (y-axis) vs log2(Agg/NonAgg) (x-axis)

Tumor DE

Agg DE

B

P(583)<7.13E-243

1329   583   437

HCC (1912)   Aggregated (1020)

	Aggregated	
	UP	DOWN
HCC UP	494	2
HCC DOWN	2	85

C

UPREGULATED GENES				DOWNREGULATED GENES			
AGGREGATED		**HCC**		**AGGREGATED**		**HCC**	
immune system process	9.05E-10	vasculature development	1.69E-09	metabolic process	4.81E-11	oxidation reduction	2.80E-51
vasculature development	4.76E-08	blood vessel development	2.47E-09	cellular ketone metabolic process	2.38E-08	metabolic process	6.14E-39
immune response	4.92E-08	angiogenesis	7.41E-09	oxidation reduction	3.59E-08	cellular ketone metabolic process	1.76E-35
blood vessel development	9.17E-08	blood vessel morphogenesis	6.77E-08	carboxylic acid metabolic process	5.46E-08	oxoacid metabolic process	5.27E-35
system development	1.93E-07	cell adhesion	1.13E-07	oxoacid metabolic process	5.46E-08	carboxylic acid metabolic process	5.27E-35
response to external stimulus	5.22E-07	biological adhesion	1.22E-07	organic acid metabolic process	5.76E-08	organic acid metabolic process	6.44E-35
anatomical structure development	1.08E-06	regulation of developmental process	2.10E-07	cellular metabolic process	5.49E-07	monocarboxylic acid metabolic process	6.63E-22
regulation of multicellular organismal process	1.86E-06	response to external stimulus	4.23E-07	cofactor metabolic process	2.96E-04	cellular metabolic process	2.41E-18
multicellular organismal development	2.34E-06	regulation of multicellular organismal process	3.24E-06	coenzyme metabolic process	4.66E-04	organic acid catabolic process	6.12E-16
response to wounding	2.51E-06	response to wounding	3.44E-06	cellular amine metabolic process	1.43E-03	carboxylic acid catabolic process	6.12E-16
extracellular region part	6.50E-20	extracellular region part	4.00E-14	intracellular part	3.51E-16	mitochondrion	5.70E-53
extracellular region	5.46E-15	extracellular matrix	1.81E-10	intracellular	4.69E-17	cytoplasm	2.43E-57
plasma membrane	2.49E-10	plasma membrane	2.64E-10	cytoplasm	6.99E-16	cytoplasmic part	9.43E-49
proteinaceous extracellular matrix	3.76E-10	proteinaceous extracellular matrix	3.81E-10	mitochondrion	1.08E-12	intracellular part	1.58E-48
extracellular matrix	3.96E-10	membrane	1.41E-09	cytoplasmic part	6.09E-11	intracellular membrane-bounded organelle	6.50E-47
extracellular space	3.39E-10	extracellular region	1.68E-09	intracellular membrane-bounded organelle	1.16E-10	membrane-bounded organelle	8.96E-47
cell surface	1.75E-07	lysosome	2.59E-09	membrane-bounded organelle	1.27E-10	intracellular	6.19E-44
plasma membrane part	1.00E-06	endoplasmic reticulum	2.63E-09	intracellular organelle	1.23E-09	mitochondrial part	8.61E-42
external side of plasma membrane	1.57E-06	lytic vacuole	3.08E-09	organelle	1.31E-09	intracellular organelle	3.77E-35
lysosome	1.32E-05	plasma membrane part	2.16E-08	mitochondrial part	1.77E-03	organelle	4.53E-35

(row labels: BIOLOGICAL PROCESS, CELLULAR COMPONENT)

D

Agg vs non-Agg   HCC vs Normal

Reln
H19
Spp1
Tff3
AFP
Tnfsf12
Tspan8
Gpc3
Spink3
Ly6d
Flt1
Cdh5
Cldn5
Cxcl9
Sdc3
Tnfrsf21
Itga9
Csf1r
Dlk1
CD44
Osmr
Cldn2
Il6st

log2(FC)   1 2 3 4 5 6

E

Ly6D   CD44   EpCAM

Cldn2   AFP   Gpc3

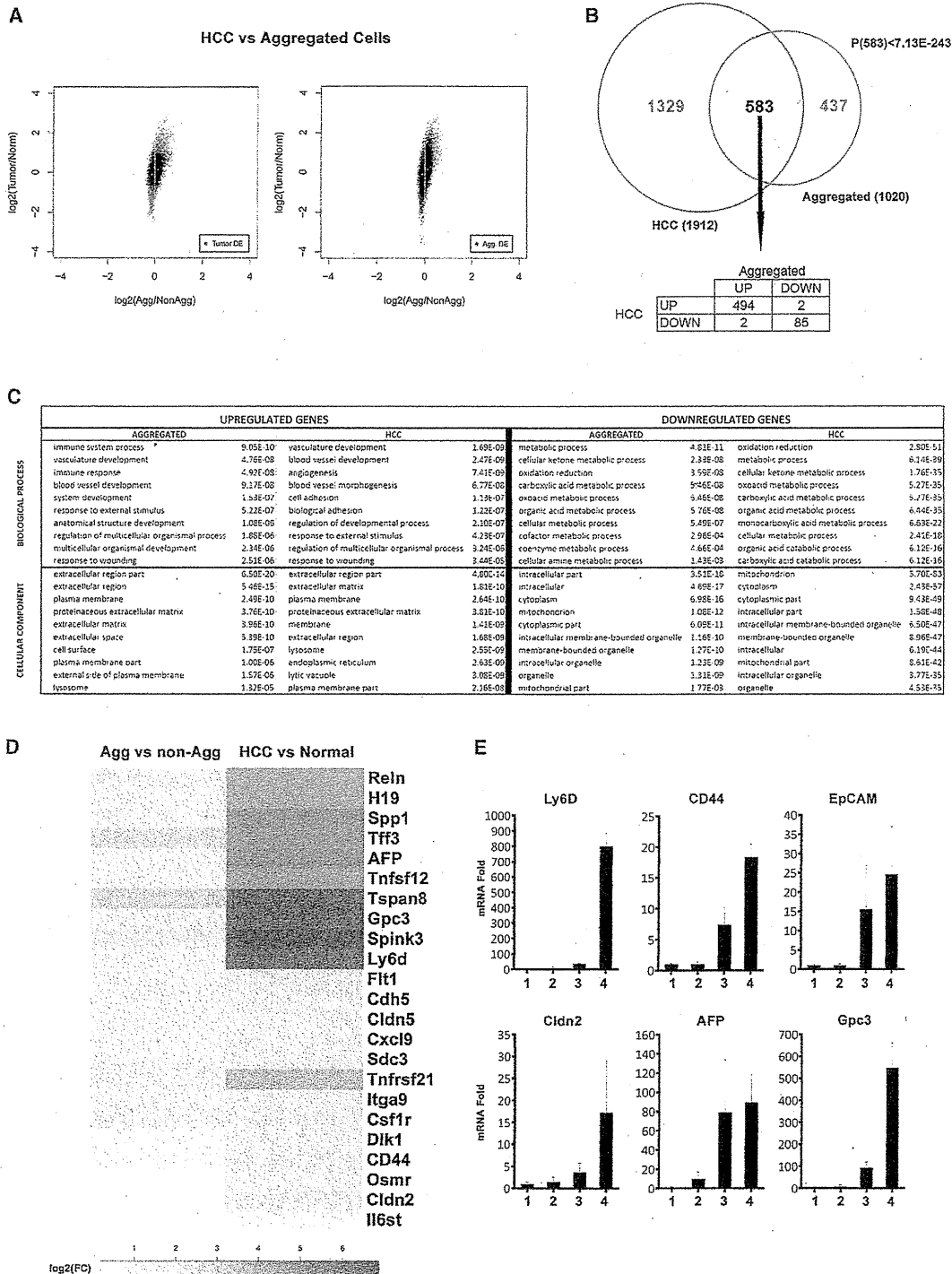(mRNA Fold, bar graphs with groups 1 2 3 4)

Figure 3. Aggregated Hepatocytes Exhibit an Altered Transcriptome Similar to that of HCC Cells

Aggregated and matched nonaggregated hepatocytes were isolated 5 months after DEN treatment. HCC cells were isolated from DEN-induced tumors, and normal hepatocytes were from age- and gender-matched control mice. RNA was extracted and subjected to microarray analysis (n = 3 for each sample).

(A) Scatterplot representing fold changes (log 2 of expression ratio) in gene expression for HCC versus normal (y axis) and aggregated versus nonaggregated (x axis) pairwise transcriptome comparisons. The plot is displayed twice: in the left panel, genes with an FDR < 0.01 in the aggregated versus nonaggregated

hepatocyte samples did not cluster with each other but rather with nonaggregated hepatocytes derived from the same mouse (Figure S3A). Interestingly, the aggregated cell transcriptome appeared closer to that of normal hepatocytes than to the HCC profile. This similarity may be due to the presence of ~70% nontumorigenic (or CD44−) hepatocytes within the purified aggregates (Figure 1D). Comparison of the HCC and normal hepatocyte transcriptomes revealed 1,912 differentially expressed genes (false discovery rate [FDR] < 0.01; Figure 3A, left, cyan dots). A similar comparison revealed 1,020 genes that are differentially expressed between aggregated and nonaggregated hepatocytes (FDR < 0.01; Figure 3A, right, red dots). The range of differential expression is wider for the HCC and normal hepatocyte pair than the aggregate versus nonaggregate pair, reflecting presence of normal, nontransformed hepatocytes within the aggregates, resulting in signal dilution. Interestingly, 57% (583/1,020) of genes differentially expressed in aggregated relative to nonaggregated hepatocytes are also differentially expressed in HCC relative to normal hepatocytes (Figure 3B, top), a value that is highly significant (p < 7.13 × 10^{-243}). More specifically, 85% (494/583) of these genes are overexpressed in both HCC and HcPC-containing aggregates (Figure 3B, bottom table). Thus, hepatocyte aggregates isolated 5 months after DEN injection contain cells that are related in their gene expression profile to HCC cells isolated from fully developed tumor nodules.

To gain insight into the functional differences between the transcriptomes of the four populations, we examined which biological processes or cellular compartments were significantly overrepresented in the induced or repressed genes in both pairwise comparisons (Gene Ontology Analysis). As expected, processes and compartments that were enriched in aggregated hepatocytes relative to nonaggregated hepatocytes were almost identical to those that were enriched in HCC relative to normal hepatocytes (Figure 3C). Upregulated genes were related to immune response, angiogenesis, development, and wound healing, and many encoded plasma membrane or secreted proteins. By contrast, downregulated genes were highly enriched for metabolic processes, and many of them encoded mitochondrial proteins or had functions associated with differentiated hepatocytes (Figure 3C). Several human HCC markers, including AFP, Gpc3 and H19, were upregulated in aggregated hepatocytes (Figures 3D and 3E). Aggregated hepatocytes also expressed more Tetraspanin 8 (Tspan8), a cell-surface glycoprotein that complexes with integrins and is overexpressed in human carci-

nomas (Zöller, 2009). Another cell-surface molecule highly expressed in aggregated cells is Ly6D (Figures 3D and 3E). Immunofluorescence (IF) analysis revealed that Ly6D was undetectable in normal liver but was elevated in FAH and ubiquitously expressed in most HCC cells (Figure S3C). A fluorescent-labeled Ly6D antibody injected into HCC-bearing mice specifically stained tumor nodules (Figure S3D). Other cell-surface molecules that were upregulated in aggregated cells included syndecan 3 (Sdc3), integrin α 9 (Itga9), claudin 5 (Cldn5), and cadherin 5 (Cdh5) (Figure 3D). Aggregated hepatocytes also exhibited elevated expression of extracellular matrix proteins (TIF3 and Reln1) and a serine protease inhibitor (Spink3). Elevated expression of such proteins may explain aggregate formation. Aggregated hepatocytes also expressed progenitor cell markers, including the epithelial cell adhesion molecule (EpCAM) (Figure 3E) and Dlk1 (Figure 3D). Elevated expression of cytokines and cytokine receptors was also detected, including tumor necrosis factor superfamily members 12 and 21, colony-stimulating factor 1 receptor, FMS-like tyrosine kinase 1, chemokine (C-X-C motif) ligand 9, the STAT3-activating cytokine osteopontin, IL-6 receptor (IL-6R) signal transducing subunit (gp130), and oncostatin M (OSM) receptor, which also activates STAT3 (Figure 3D).

Aggregated hepatocytes expressed albumin, albeit less than nonaggregated hepatocytes (Figure 4A). Some aggregated cells were positive for cytokeratin 19 (CK19) and A6, markers for bile duct epithelium and oval cells (Figure 4A). Most cells in the DEN-induced aggregates were AFP positive, and some of them expressed EpCAM (Figure 4A). However, not all markers were expressed by every cell within a given aggregate, suggesting that the aggregates contain liver cells that are related to bipotential hepatobiliary progenitors/oval cells as well as more differentiated progeny and normal hepatocytes. To confirm these observations, we compared the HcPC and HCC (Figure 3A) to the transcriptome of DDC-induced oval cells (Shin et al., 2011). This analysis revealed a striking similarity between the HCC, HcPC, and the oval cell transcriptomes (Figure S3B). Despite these similarities, some genes that were upregulated in HcPC-containing aggregates and HCC were not upregulated in oval cells. Such genes may account for the tumorigenic properties of HcPC and HCC.

We examined the aggregates for signaling pathways and transcription factors involved in hepatocarcinogenesis. Many aggregated cells were positive for phosphorylated c-Jun and STAT3 (Figure 4A), transcription factors involved in DEN-induced

comparison are highlighted in red, and in the right panel, genes with an FDR < 0.01 in the HCC versus normal comparison are highlighted in cyan. DE, differentially expressed.

(B) Venn diagram showing overlap between genes that are differentially expressed between aggregated and nonaggregated hepatocytes and between HCC cells and normal hepatocytes with an FDR < 0.01 (cyan and red dots from A). The probability to find 583 overlapping genes is <7.13 × 10^{-243}. From these 583 common genes, only 4 behaved differently.

(C) The ten most enriched biological processes (upper table) and cellular compartments (lower panel) represented by genes that are significantly upregulated (left panel) or downregulated (right panel) in HCC relative to normal hepatocytes (HCC) or in aggregated relative to nonaggregated hepatocytes (aggregated).

(D) Heatmap displaying positive fold changes (FC) in expression of genes of interest in aggregated versus nonaggregated HcPCs (left) and in HCC versus normal hepatocytes (right).

(E) Expression of selected genes was examined by real-time PCR and is depicted as fold change relative to normal hepatocytes given an arbitrary value of 1.0 (n = 3; ± SD). (1) Normal hepatocytes; (2) nonaggregated hepatocytes from DEN-treated liver; (3) HcPC aggregates from DEN-treated liver; and (4) DEN-induced HCCs.
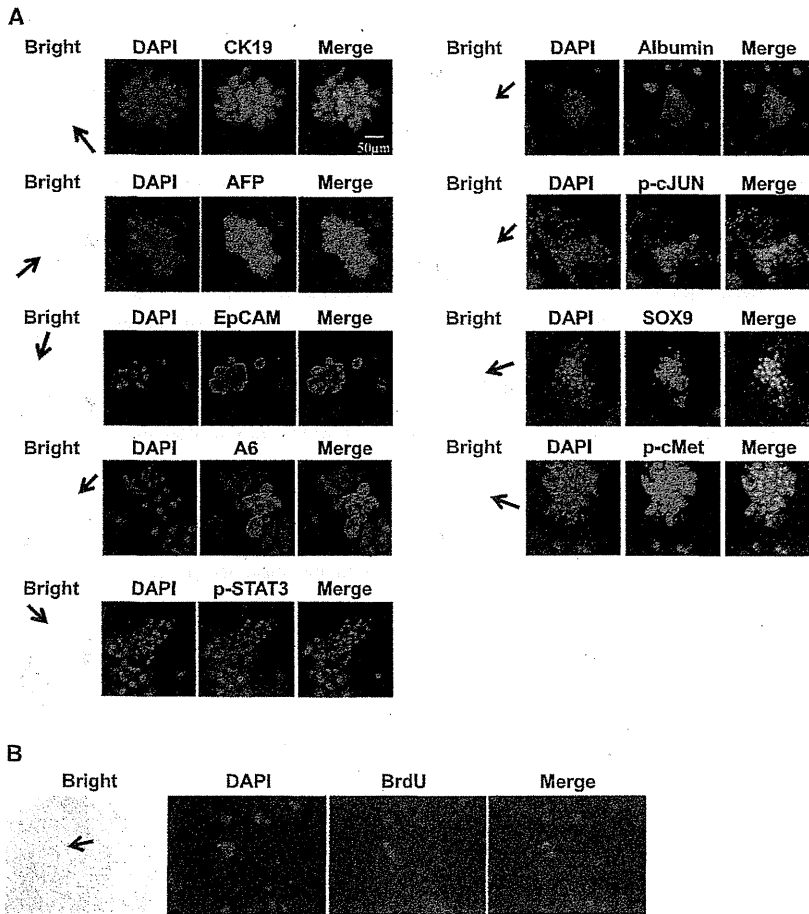
See also Figure S3.

A

B

Figure 4. DEN-Induced HcPC Aggregates Express Pathways and Markers Characteristic of HCC and Hepatobiliary Stem Cells

(A) Cytospin preps of collagenase-resistant aggregates from 5-month-old DEN-injected mice were stained with antibodies to CK19, AFP, EpCAM, A6, phospho-Y-STAT3 (Tyr705), albumin, phospho-c-Jun, Sox9, and phospho-c-Met. Black arrows indicate aggregates, and yellow arrows indicate nonaggregated cells (magnification: 400×).
(B) 5-month-old DEN-treated mice were injected with BrdU, and 2 hr later, collagenase-resistant aggregates were isolated and analyzed for BrdU incorporation (400×).
See also Figure S4.

HcPC-Containing Aggregates Originate from Premalignant Dysplastic Lesions

FAH are dysplastic lesions occurring in rodent livers exposed to hepatic carcinogens (Su et al., 1990). Similar lesions are present in premalignant human livers (Su et al., 1997). Yet, it is still debated whether FAH correspond to premalignant lesions or are a reaction to liver injury that does not lead to cancer (Sell and Leffert, 2008). In DEN-treated males, FAH were detected as early as 3 months after DEN administration (Figure 5A), concomitant with the time at which HcPC-containing aggregates were detected. In females, FAH development was delayed. In both genders, FAH

hepatocarcinogenesis (Eferl et al., 2003; He et al., 2010). Sox9, a transcription factor that marks hepatobiliary progenitors (Dorrell et al., 2011), was also expressed by many of the aggregated cells, which were also positive for phosphorylated c-Met (Figure 4A), a receptor tyrosine kinase that is activated by hepatocyte growth factor (HGF) and is essential for liver development (Bladt et al., 1995) and hepatocarcinogenesis (Wang et al., 2001). Few of the nonaggregated hepatocytes exhibited activation of these signaling pathways. Aggregates from bromodeoxyuridine (BrdU)-pulsed DEN-treated mice contained BrdU-positive cells (Figure 4B), indicating that they were actively proliferating prior to isolation. Hepatocyte aggregates from 1-month-old Tak1$^{\Delta hep}$ mice also contained cells positive for AFP, Sox9, phosphorylated c-Met, and EpCAM, but not A6-positive cells (Figure S4A). Many of the cells also exhibited partially activated β-catenin, phosphorylated STAT3, and phosphorylated c-Jun. Thus, despite different etiology, HcPC-containing aggregates from Tak1$^{\Delta hep}$ mice exhibit upregulation of many of the same markers and pathways that are upregulated in DEN-induced HcPC-containing aggregates. Flow cytometry confirmed enrichment of CD44$^+$ cells as well as CD44$^+$/CD90$^+$ and CD44$^+$/EpCAM$^+$ double-positive cells in the HcPC-containing aggregates from either DEN-treated or Tak1$^{\Delta hep}$ livers (Figure S4B).

were confined to zone 3 and consisted of tightly packed small hepatocytic cells, some of which were proliferative based on BrdU incorporation (Figure 5B). BrdU$^+$ cells were first detected in DEN-treated males and were confined to FAH and rarely detected in age-matched control mice. FAH contained cells positive for the same progenitor cell markers and activated signaling pathways present in HcPC-containing aggregates, including AFP, CD44, and EpCAM (Figure 5C). FAH also contained cells positive for activated STAT3, c-Jun, and PCNA (Figure 5C). Many cells within FAH exhibited strong upregulation of YAP (Figure 5C), a transcriptional coactivator that is negatively regulated by the Hippo pathway and a liver cancer oncoprotein (Zheng et al., 2011). FAH were also enriched in F4/80$^+$ macrophages (Figure 5C). These results suggest that the HcPC-containing aggregates may be derived from FAH.

HcPCs Exhibit Autocrine IL-6 Expression Necessary for HCC Progression

In situ hybridization (ISH) and immunohistochemistry (IHC) revealed that DEN-induced FAH contained IL-6-expressing cells (Figures 6A, 6B, and S5), and freshly isolated DEN-induced aggregates contained more IL-6 messenger RNA (mRNA) than nonaggregated hepatocytes (Figure 6C). We examined several
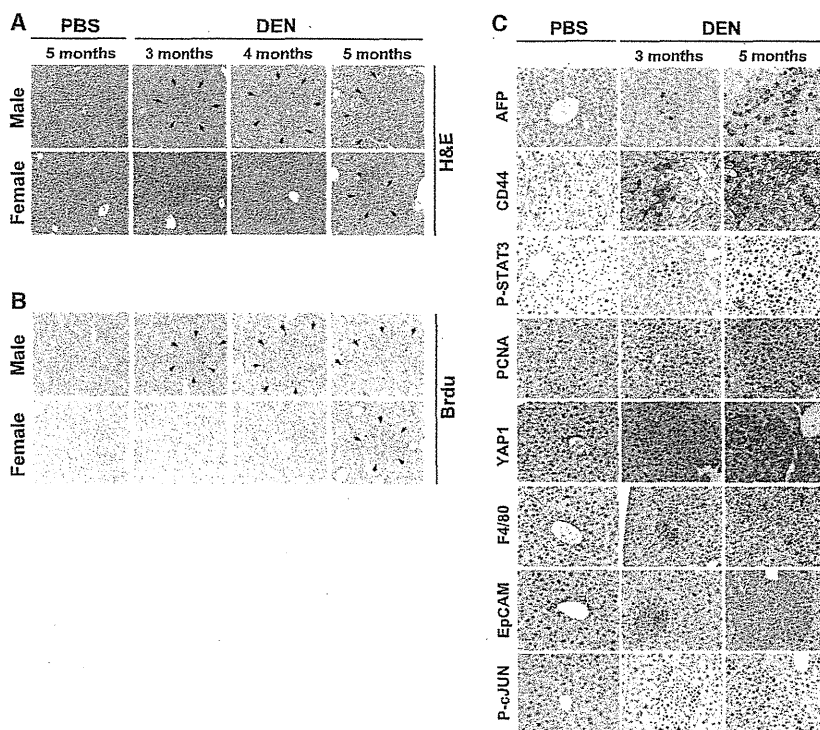
A

B

C

Figure 5. HcPC-Containing Aggregates May Originate from Liver Premalignant Lesions
(A and B) Male and female mice were injected with PBS or DEN at 15 days. At the indicated time points, BrdU was administrated, and livers were collected 2 hr later and stained with H&E (A) or a BrdU-specific antibody (B). Arrows indicate borders of FAH (magnification: 200×).
(C) Sections of male livers treated as above were subjected to IHC with the indicated antibodies (400×).

IL-6 deficiency resulted in a 2.5-fold decrease in tumorigenic potential (Figure 7C), suggesting that autocrine IL-6 contributes to HcPC to HCC progression. To confirm this point, we dispersed freshly isolated DEN-induced aggregates and transduced them with bicistronic lentiviruses encoding either scrambled or IL-6-specific shRNAs and a GFP marker. After a few days in culture, the transduced cells were introduced into MUP-uPA mice that were examined for HCC development 6 months later. Silencing of IL-6 reduced HCC generation (Figure 7D) and inhibited formation of GFP⁺ colonies

factors that control IL-6 expression and found that LIN28A and B were significantly upregulated in HcPCs and HCC (Figures 6D and 6E). LIN28-expressing cells were also detected within FAH (Figure 6F). As reported (Iliopoulos et al., 2009), knockdown of LIN28B in cultured HcPC or HCC cell lines decreased IL-6 expression (Figure 6G). LIN28 exerts its effects through downregulation of the microRNA (miRNA) Let-7 (Iliopoulos et al., 2009). Accordingly, miRNA array analysis of aggregated and nonaggregated hepatocytes from DEN-treated mice indicated that the amount of Let-7, along with other miRNAs that also inhibit IL-6 expression (miR194 and miR872), was lower in aggregated cells than in nonaggregated cells (Table S2).

To determine whether autocrine IL-6 production is needed for HCC growth, we silenced IL-6 expression with small hairpin RNA (shRNA) in dih10 HCC cells (He et al., 2010). This resulted in nearly a 75% decrease in IL-6 mRNA (Figure 7A) but had little effect on cell growth in the presence of growth factors, including EGF and insulin (Figure S6A). IL-6 mRNA silencing, however, diminished the ability of dih10 cells to form s.c. tumors (Figures S6B and S6C) and inhibited their ability to form HCCs and proliferate after transplantation into MUP-uPA mice (Figures 7B and S6D). To investigate the importance of autocrine IL-6 production at an earlier step, we isolated HcPC from DEN-treated WT and $Il6^{-/-}$ mice. Although IL-6 ablation attenuates HCC induction (Naugler et al., 2007), we still could isolate collagenase-resistant aggregates from livers of DEN-injected $Il6^{-/-}$ mice. Notably, IL-6 ablation did not reduce the proportion of CD44⁺ cells in the aggregates (Figures S7A and S7B). We introduced an identical number of WT and $Il6^{-/-}$ aggregated hepatocytes into MUP-uPA mice and scored HCC development 5 months later. The

within the MUP-uPA liver (Figure 7E). We also ablated IL-6 expression in mouse hepatocytes and found that this led to a marked reduction in DEN-induced tumorigenesis (Figure 7F). Thus, autocrine IL-6 production by DEN-initiated HcPC is important for HCC development. To investigate whether autocrine IL-6 signaling also occurs in human premalignant lesions, we examined needle biopsies of normal liver tissue and HCV-infected livers with dysplastic lesions. We found that 16% of all (n = 25) dysplastic lesions exhibited coexpression of LIN28 and IL-6 and contained activated STAT3 (Figure 7G). These markers were hardly detected in normal liver or nontumor portion of HCV-infected livers.

DISCUSSION

The isolation and characterization of cells that can give rise to HCC only after transplantation into an appropriate host liver undergoing chronic injury demonstrates that cancer arises from progenitor cells that are yet to become fully malignant. Importantly, unlike fully malignant HCC cells, the HcPCs we isolated cannot form s.c. tumors or even liver tumors when introduced into a nondamaged liver. Liver damage induced by uPA expression or CCl₄ treatment provides HcPCs with the proper cytokine and growth factor milieu needed for their proliferation. Although HcPCs produce IL-6, they may also depend on other cytokines such as TNF, which is produced by macrophages that are recruited to the damaged liver. In addition, uPA expression and CCl₄ treatment may enhance HcPC growth and progression through their fibrogenic effect on hepatic stellate cells. Although HCC and other cancers have been suspected to arise from
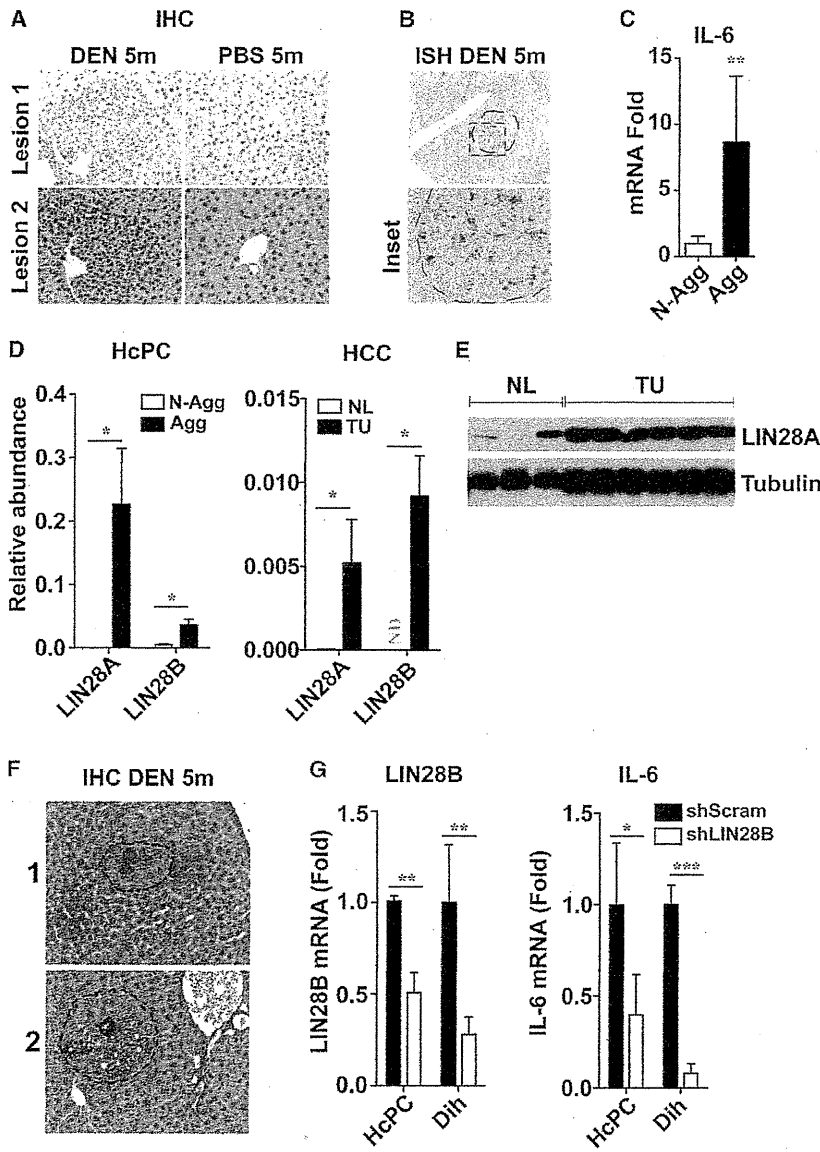
A IHC
DEN 5m PBS 5m
Lesion 1
Lesion 2

B ISH DEN 5m
Inset

C IL-6
mRNA Fold
15
10
5
0
N-Agg Agg

D HcPC
Relative abundance
0.4
0.3
0.2
0.1
0.0
□N-Agg ■Agg
LIN28A LIN28B

HCC
0.015
0.010
0.005
0.000
□NL ■TU
LIN28A LIN28B

E
NL TU
LIN28A
Tubulin

F IHC DEN 5m
1
2

G LIN28B
LIN28B mRNA (Fold)
1.5
1.0
0.5
0.0
HcPC Dih

IL-6
IL-6 mRNA (Fold)
1.5
1.0
0.5
0.0
■shScram □shLIN28B
HcPC Dih

Figure 6. Liver Premalignant Lesions and HcPCs Exhibit Elevated IL-6 and LIN28 Expression

(A and B) Livers of 5-month-old DEN injected mice were analyzed for IL-6 expression by IHC (magnification: 400×) (A) and ISH (magnification: 100×, top; 400×, bottom) (B).

(C and D) Quantification of IL-6 (C) and LIN28 (D) mRNA in aggregated versus nonaggregated hepatocytes from 5-month-old DEN-treated livers and in normal versus tumor-bearing livers (n = 6; ± SEM) (ND, not detected).

(E) Immunoblot analyses of LIN28A in normal (NL) and tumor-bearing (TU) livers.

(F) DEN-treated livers were subjected to IHC with a LIN28A antibody. Broken lines indicate borders of FAH (400×).

(G) LIN28B was silenced with shRNA in HCC (dih) cells and cultured HcPCs, and LIN28B and IL-6 mRNAs were quantitated by qRT-PCR (n = 3; ± SEM).

See also Figure S5 and Table S2.

dysplastic lesions and mouse FAH and HcPC exhibit autocrine IL-6 signaling. HcPC are not unique to DEN-treated mice, and similar cells were isolated from Tak1$^{\Delta hep}$ mice in which HCC development resembles cirrhosis-associated human HCC (Inokuchi et al., 2010).

HcPC Origin and Relationship to Liver and HCC Stem Cells

Transcriptomic analysis indicates that DEN-induced HcPCs are related to both normal hepatobiliary bipotential stem cells/oval cells and HCC cells. Although HcPCs are not fully transformed, they express several markers—CD44, EpCAM, AFP, SOX9, OV6, and CK19—found to be expressed by HCC stem cells and oval cells (Guo et al., 2012; Mikhail and He, 2011; Terris et al., 2010; Yamashita et al., 2008; Zhu et al., 2010). However,

premalignant/dysplastic lesions (Hruban et al., 2007; Hytiroglou et al., 2007), a direct demonstration that such lesions progress into malignant tumors has been lacking. Based on expression of common markers—EpCAM, CD44, AFP, activated STAT3, and IL-6—that are not expressed in normal hepatocytes, we postulate that HcPCs originate from FAH or dysplastic foci, which are first observed in male mice within 3 months of DEN exposure. Indeed, the cells that are contained within the FAH are smaller than the surrounding parenchyma and are similar in size to isolated HcPCs. Importantly, FAH or premalignant dysplastic foci are not unique to DEN-treated rodents (Bannasch, 1984; Rabes, 1983), and similar lesions were detected in human cirrhotic livers (Hytiroglou et al., 2007; Seki et al., 2000; Takayama et al., 1990) in which the rate of HCC progression is 3%–5% per year (El-Serag, 2011). We found that human

unlike oval cells, which do not express albumin or AFP and do not give rise to liver tumors upon transplantation into MUP-uPA mice, HcPCs give rise to HCC after intrasplenic transplantation. Yet, unlike dih10 HCC cells, which express high levels of the HCC stem cell markers AFP, CD44, and EpCAM, HcPCs do not form s.c. tumors.

At this point, it is not clear whether HcPCs arise from oval cells or from dedifferentiated hepatocytes. Given that DEN is metabolically activated by Cyp2E1 that is expressed only in fully differentiated zone 3 hepatocytes (Tsutsumi et al., 1989) and that Cyp2E1$^{-/-}$ mice are refractory to DEN (Kang et al., 2007), DEN-induced HcPC are most likely derived from dedifferentiated hepatocytes. Consistent with this hypothesis, DEN-induced FAH and proliferating cells were found in zone 3 and not near bile ducts or the canals of Hering, sites at which oval cells reside
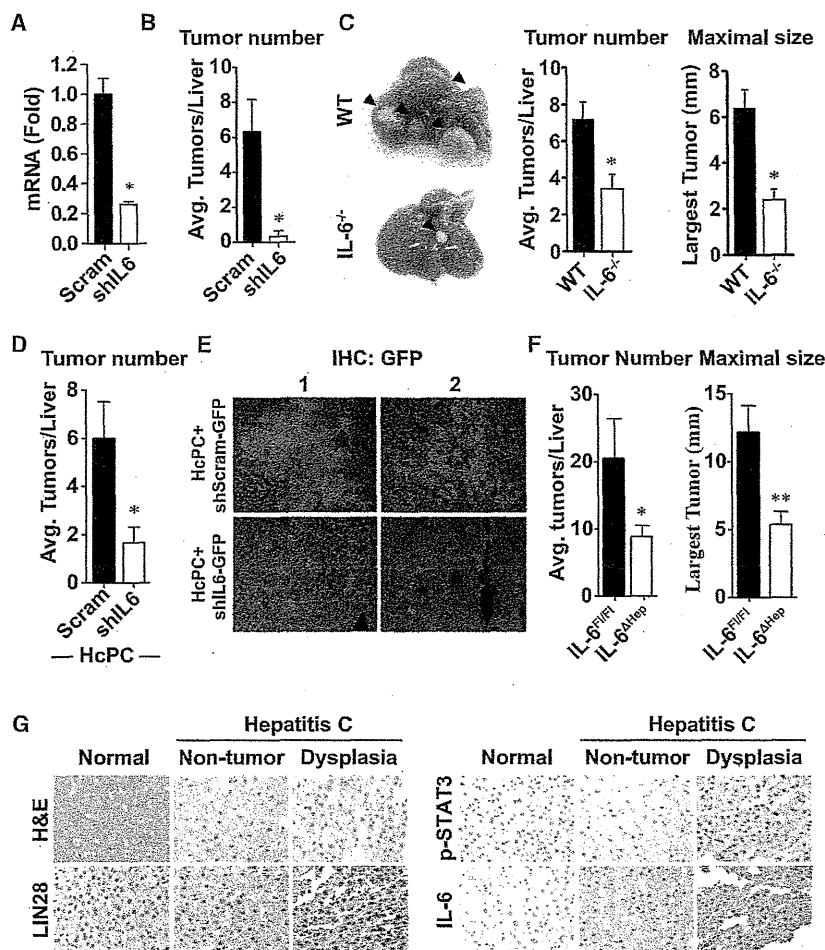
Figure 7. HCC Growth Depends on Autocrine IL-6 Production

(A) HCC cells (dih10) were transduced with lentiviruses containing scrambled or IL-6-specific shRNA. IL-6 mRNA was analyzed by qRT-PCR.

(B) Dih10 cells (1.2×10^5) transduced as above were i.s. injected into MUP-uPA mice that were analyzed 6 months later for HCC development (n = 3; ± SEM).

(C) HcPCs from WT and $Il6^{-/-}$ mice were injected (1×10^4 cells/mice) into MUP-uPA mice and analyzed 5 months later for HCC development (n = 5; ± SEM).

(D) HcPCs isolated from DEN-treated WT mice were transduced with shRNA against IL-6 or scrambled shRNA, cultured for 3 to 4 days, i.s. transplanted (1×10^4 cells/mice) into MUP-uPA mice, and analyzed 6 months later (n = 3; ± SEM).

(E) Livers of MUP-uPA mice from (D) were immunostained with GFP antibody 6 months after transplantation (200×). The bicistronic lentivirus in this experiment expresses GFP along with control or IL-6 shRNA, allowing tracking of the infected cells.

(F) DEN-treated $Il6^{\Delta hep}$ and $Il6^{F/F}$ mice were sacrificed after 9 months to evaluate tumor multiplicity and size (n = 6–10, ± SEM).

(G) IHC analysis of autocrine IL-6 signaling in human premalignant lesions in HCV-infected livers. Expression of LIN28, p-STAT3, and IL-6 was analyzed in 25 needle biopsies of dysplastic nodules, and representative positive specimens (n = 4) are shown. The dysplastic nodules and paired nontumor tissue were obtained from the same HCV-infected patient (n = 25). Nontumor tissue of metastatic liver cancer was used as normal control.

See also Figures S6 and S7.

(Duncan et al., 2009). Notably, GO analysis revealed that many of the genes whose expression is downregulated in HcPC-containing aggregates are involved in xenobiotic and organic acid metabolism, characteristics of differentiated hepatocytes. The same types of genes are also downregulated in HCC. However, final identification of the origin of HcPC will be provided by ongoing lineage-tracing experiments.

The Significance of Autocrine IL-6 Expression

Elevated IL-6 was detected in at least 40% of human HCCs, where it is expressed by the cancer cells (Soresi et al., 2006). More recent studies have confirmed upregulation of IL-6 in human HCC and suggested that it plays a central role in a gene expression network that drives tumor development (Ji et al., 2009). Elevated IL-6 was also found in viral and alcoholic hepatitis and liver cirrhosis, but in these conditions, IL-6 is expressed mainly by myeloid cells/leukocytes rather than parenchymal cells (Deviere et al., 1989; Kakumu et al., 1993; Soresi et al., 2006). Our studies indicate that the critical site of IL-6 expression shifts from myeloid cells to epithelial cells during the course of DEN-induced liver tumorigenesis. Initially, DEN administration rapidly induces IL-6 in Kupffer cells through NF-κB activation

(Maeda et al., 2005). This initial surge in IL-6 is required for DEN-induced hepatocarcinogenesis (Naugler et al., 2007). Although IL-6 decays within 2 weeks of DEN administration, it reappears several months later, but at that time, it is expressed within FAH. IL-6 expression is also elevated in isolated HcPCs and is maintained in fully transformed HCC cells. Furthermore, autocrine IL-6 is important for HcPC to HCC progression and for tumorigenic growth. Autocrine IL-6 in both HcPC and HCC cells depends on elevated expression of LIN28, an RNA-binding protein that exerts its protumorigenic activity through downregulation of Let-7, an miRNA that inhibits IL-6 expression (Viswanathan and Daley, 2010). Accordingly, HcPCs exhibit downregulation of both Let-7f and Let-7g, and elevated LIN28 is found not only in isolated HcPCs but also within FAH and human HCV-induced dysplastic lesions.

A similar LIN28-Let-7-IL-6 epigenetic switch is important for in vitro programming and maintenance of cancer stem cells (Iliopoulos et al., 2009). IL-6 also induces malignant features in human ductal carcinoma stem cells (Sansone et al., 2007). In fact, autocrine IL-6 signaling was suggested to play a key role in STAT3-dependent tumor progression (Grivennikov and Karin, 2008). Another miRNA-driven autoregulatory circuit involved in

hepatocarcinogenesis accounts for elevated IL-6R expression (Hatziapostolou et al., 2011). Yet, HcPC-containing aggregates also express several other STAT3-activiting cytokines and receptors. Accordingly, silencing or ablation of IL-6 results in incomplete inhibition of HcPC to HCC progression. Nonetheless, our results demonstrate that autoregulatory circuits/epigenetic switches play an important role in the very early stages of tumorigenesis. Given that such circuits are already activated in premalignant cells, pharmacological agents that disrupt their function may be useful in cancer prevention. Prevention is of particular importance in cancers such as HCC, which is often detected at a stage that is refractory to currently available therapeutics.

EXPERIMENTAL PROCEDURES

Mice, HCC Induction, HcPC Isolation, and Transplantation

MUP-uPA transgenic mice (Weglarz et al., 2000) were maintained on a pure BL/6 background. Because homozygous females frequently die when pregnant, MUP-uPA heterozygotes were generated by backcrossing homozygous MUP-uPA males with BL/6 females to be used as recipients for hepatic transplantation. $Tak1^{\Delta hep}$ (Inokuchi et al., 2010) and $Il6^{F/F}$ (Quintana et al., 2013) mice were also in the BL/6 background. $Il6^{\Delta hep}$ mice were generated by crossing $Il6^{F/F}$ and Alb-Cre mice. C57BL/6 actin-GFP mice were from the Jackson Laboratories. BL/6 mice were purchased from Charles River Laboratories.

To induce HCC, 15-day-old mice were injected i.p. with 25 mg/kg DEN (Sigma). A pool of DEN-injected BL/6 mice was maintained and used in most experiments. Hepatocytes were isolated using a two-step procedure (He et al., 2010). Cell aggregates were isolated by filtration through 70 and 40 μm sieves. To disperse the aggregates into single cells, they were subjected to gentle pipetting in Ca/Mg-free PBS on ice. Single-cell suspensions of aggregated and nonaggregated hepatocytes were transplanted via an i.s. injection into 21-day-old male MUP-uPA mice (He et al., 2010). Alternatively, single-cell suspensions of aggregated hepatocytes were enriched for CD44$^+$ HcPC using magnetic beads. As few as 100 viable CD44$^+$ cells mixed with 1 × 10^5 normal hepatocytes from normal males were transplanted into MUP-uPA mice. Alternatively, BL/6 mice were pretreated with retrorsine (70 mg/kg i.p.) (Sigma), a cell-cycle inhibitor, 1 month prior to transplantation. Transplanted mice were allowed to recover for 1 week and then injected weekly with 3× 0.5 ml/kg CCl$_4$ i.p. to induce liver injury and hepatocyte proliferation (Guo et al., 2002). Mice were sacrificed 5 to 6 months later, and tumors bigger than 1 mm in diameter on the liver surface were counted. Tumors bigger than 5 mm across were dissected for biochemical and molecular analyses.

ACCESSION NUMBERS

Raw gene expression array data have been deposited to NCBI's Gene Expression Omnibus under the GSE50431 study.

SUPPLEMENTAL INFORMATION

Supplemental Information includes Extended Experimental Procedures, seven figures, and three tables and can be found with this article online at http://dx.doi.org/10.1016/j.cell.2013.09.031.

AUTHOR CONTRIBUTIONS

G.H. identified, isolated, and characterized HcPCs; D.D. and H.N. optimized the HcPC isolation and purification procedure; D.D. found the mechanism of their dependence on autocrine IL-6 controlled by LIN28, characterized them using flow cytometry (with S.S.), and conducted miR analyses (with M.H. and D.I.); H.N. and D.D. used $Il6^{\Delta hep}$ mice to demonstrate in vivo HCC dependency on autocrine IL-6; H.N. (with R.T. and K.K.) found IL-6, LIN28, and P-STAT3 in human dysplastic lesions; J.F.-B. conducted the transcriptome

analysis and exome sequencing (with S.E.Y., K.J., and O.H.) and with H.O. examined oncogenic potential of oval cells; H.O. examined HcPC proliferative potential and performed IF analysis of isolated HcPC (with A.S. and R.M.H.); Y.J. assisted with IHC and ISH staining; E.S. contributed to the experiments involving $Tak1^{\Delta hep}$ mice; G.H., D.D., J.F.-B., H.O., and M.K. wrote the manuscript.

REFERENCES

Bannasch, P. (1984). Sequential cellular changes during chemical carcinogenesis. J. Cancer Res. Clin. Oncol. 108, 11–22.

Bladt, F., Riethmacher, D., Isenmann, S., Aguzzi, A., and Birchmeier, C. (1995). Essential role for the c-met receptor in the migration of myogenic precursor cells into the limb bud. Nature 376, 768–771.

Deviere, J., Content, J., Denys, C., Vandenbussche, P., Schandene, L., Wybran, J., and Dupont, E. (1989). High interleukin-6 serum levels and increased production by leucocytes in alcoholic liver cirrhosis. Correlation with IgA serum levels and lymphokines production. Clin. Exp. Immunol. 77, 221–225.

Dorrell, C., Erker, L., Schug, J., Kopp, J.L., Canaday, P.S., Fox, A.J., Smirnova, O., Duncan, A.W., Finegold, M.J., Sander, M., et al. (2011). Prospective isolation of a bipotential clonogenic liver progenitor cell in adult mice. Genes Dev. 25, 1193–1203.

Duncan, A.W., Dorrell, C., and Grompe, M. (2009). Stem cells and liver regeneration. Gastroenterology 137, 466–481.

Eferl, R., Ricci, R., Kenner, L., Zenz, R., David, J.P., Rath, M., and Wagner, E.F. (2003). Liver tumor development. c-Jun antagonizes the proapoptotic activity of p53. Cell 112, 181–192.

El-Serag, H.B. (2011). Hepatocellular carcinoma. N. Engl. J. Med. 365, 1118–1127.

Grivennikov, S., and Karin, M. (2008). Autocrine IL-6 signaling: a key event in tumorigenesis? Cancer Cell 13, 7–9.

Guichard, C., Amaddeo, G., Imbeaud, S., Ladeiro, Y., Pelletier, L., Maad, I.B., Calderaro, J., Bioulac-Sage, P., Letexier, M., Degos, F., et al. (2012). Integrated analysis of somatic mutations and focal copy-number changes identifies key genes and pathways in hepatocellular carcinoma. Nat. Genet. 44, 694–698.

Guo, D., Fu, T., Nelson, J.A., Superina, R.A., and Soriano, H.E. (2002). Liver repopulation after cell transplantation in mice treated with retrorsine and carbon tetrachloride. Transplantation 73, 1818–1824.
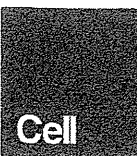
Guo, X., Xiong, L., Sun, T., Peng, R., Zou, L., Zhu, H., Zhang, J., Li, H., and Zhao, J. (2012). Expression features of SOX9 associate with tumor progression and poor prognosis of hepatocellular carcinoma. Diagn. Pathol. *7*, 44.

Haridass, D., Yuan, Q., Becker, P.D., Cantz, T., Iken, M., Rothe, M., Narain, N., Bock, M., Nörder, M., Legrand, N., et al. (2009). Repopulation efficiencies of adult hepatocytes, fetal liver progenitor cells, and embryonic stem cell-derived hepatic cells in albumin-promoter-enhancer urokinase-type plasminogen activator mice. Am. J. Pathol. *175*, 1483–1492.

Hatziapostolou, M., Polytarchou, C., Aggelidou, E., Drakaki, A., Poultsides, G.A., Jaeger, S.A., Ogata, H., Karin, M., Struhl, K., Hadzopoulou-Cladaras, M., and Iliopoulos, D. (2011). An HNF4α-miRNA inflammatory feedback circuit regulates hepatocellular oncogenesis. Cell *147*, 1233–1247.

He, G., Yu, G.Y., Temkin, V., Ogata, H., Kuntzen, C., Sakurai, T., Sieghart, W., Peck-Radosavljevic, M., Leffert, H.L., and Karin, M. (2010). Hepatocyte IKKbeta/NF-kappaB inhibits tumor promotion and progression by preventing oxidative stress-driven STAT3 activation. Cancer Cell *17*, 286–297.

Hruban, R.H., Maitra, A., Kern, S.E., and Goggins, M. (2007). Precursors to pancreatic cancer. Gastroenterol. Clin. North Am. *36*, 831–849, vi.

Hytiroglou, P., Park, Y.N., Krinsky, G., and Theise, N.D. (2007). Hepatic precancerous lesions and small hepatocellular carcinoma. Gastroenterol. Clin. North Am. *36*, 867–887, vii.

Ichinohe, N., Kon, J., Sasaki, K., Nakamura, Y., Ooe, H., Tanimizu, N., and Mitaka, T. (2012). Growth ability and repopulation efficiency of transplanted hepatic stem cells, progenitor cells, and mature hepatocytes in retrorsine-treated rat livers. Cell Transplant. *21*, 11–22.

Iliopoulos, D., Hirsch, H.A., and Struhl, K. (2009). An epigenetic switch involving NF-kappaB, Lin28, Let-7 MicroRNA, and IL6 links inflammation to cell transformation. Cell *139*, 693–706.

Inokuchi, S., Aoyama, T., Miura, K., Osterreicher, C.H., Kodama, Y., Miyai, K., Akira, S., Brenner, D.A., and Seki, E. (2010). Disruption of TAK1 in hepatocytes causes hepatic injury, inflammation, fibrosis, and carcinogenesis. Proc. Natl. Acad. Sci. USA *107*, 844–849.

Ji, J., Shi, J., Budhu, A., Yu, Z., Forgues, M., Roessler, S., Ambs, S., Chen, Y., Meltzer, P.S., Croce, C.M., et al. (2009). MicroRNA expression, survival, and response to interferon in liver cancer. N. Engl. J. Med. *361*, 1437–1447.

Kakumu, S., Shinagawa, T., Ishikawa, T., Yoshioka, K., Wakita, T., and Ida, N. (1993). Interleukin 6 production by peripheral blood mononuclear cells in patients with chronic hepatitis B virus infection and primary biliary cirrhosis. Gastroenterol. Jpn. *28*, 18–24.

Kang, J.S., Wanibuchi, H., Morimura, K., Gonzalez, F.J., and Fukushima, S. (2007). Role of CYP2E1 in diethylnitrosamine-induced hepatocarcinogenesis in vivo. Cancer Res. *67*, 11141–11146.

Laconi, E., Oren, R., Mukhopadhyay, D.K., Hurston, E., Laconi, S., Pani, P., Dabeva, M.D., and Shafritz, D.A. (1998). Long-term, near-total liver replacement by transplantation of isolated hepatocytes in rats treated with retrorsine. Am. J. Pathol. *153*, 319–329.

Maeda, S., Kamata, H., Luo, J.L., Leffert, H., and Karin, M. (2005). IKKbeta couples hepatocyte death to cytokine-driven compensatory proliferation that promotes chemical hepatocarcinogenesis. Cell *121*, 977–990.

Marquardt, J.U., and Thorgeirsson, S.S. (2010). Stem cells in hepatocarcinogenesis: evidence from genomic data. Semin. Liver Dis. *30*, 26–34.

Meyer, K., Lee, J.S., Dyck, P.A., Cao, W.Q., Rao, M.S., Thorgeirsson, S.S., and Reddy, J.K. (2003). Molecular profiling of hepatocellular carcinomas developing spontaneously in acyl-CoA oxidase deficient mice: comparison with liver tumors induced in wild-type mice by a peroxisome proliferator and a genotoxic carcinogen. Carcinogenesis *24*, 975–984.

Mikhail, S., and He, A.R. (2011). Liver cancer stem cells. Int. J. Hepatol. *2011*, 486954.

Naugler, W.E., Sakurai, T., Kim, S., Maeda, S., Kim, K., Elsharkawy, A.M., and Karin, M. (2007). Gender disparity in liver cancer due to sex differences in MyD88-dependent IL-6 production. Science *317*, 121–124.

Nguyen, L.V., Vanner, R., Dirks, P., and Eaves, C.J. (2012). Cancer stem cells: an evolving concept. Nat. Rev. Cancer *12*, 133–143.

Nowell, P.C. (1976). The clonal evolution of tumor cell populations. Science *194*, 23–28.

Park, E.J., Lee, J.H., Yu, G.Y., He, G., Ali, S.R., Holzer, R.G., Osterreicher, C.H., Takahashi, H., and Karin, M. (2010). Dietary and genetic obesity promote liver inflammation and tumorigenesis by enhancing IL-6 and TNF expression. Cell *140*, 197–208.

Pitot, H.C. (1990). Altered hepatic foci: their role in murine hepatocarcinogenesis. Annu. Rev. Pharmacol. Toxicol. *30*, 465–500.

Porta, C., De Amici, M., Quaglini, S., Paglino, C., Tagliani, F., Boncimino, A., Moratti, R., and Corazza, G.R. (2008). Circulating interleukin-6 as a tumor marker for hepatocellular carcinoma. Ann. Oncol. *19*, 353–358.

Quintana, A., Erta, M., Ferrer, B., Comes, G., Giralt, M., and Hidalgo, J. (2013). Astrocyte-specific deficiency of interleukin-6 and its receptor reveal specific roles in survival, body weight and behavior. Brain Behav. Immun. *27*, 162–173.

Rabes, H.M. (1983). Development and growth of early preneoplastic lesions induced in the liver by chemical carcinogens. J. Cancer Res. Clin. Oncol. *106*, 85–92.

Rhim, J.A., Sandgren, E.P., Degen, J.L., Palmiter, R.D., and Brinster, R.L. (1994). Replacement of diseased mouse liver by hepatic cell transplantation. Science *263*, 1149–1152.

Sansone, P., Storci, G., Tavolari, S., Guarnieri, T., Giovannini, C., Taffurelli, M., Ceccarelli, C., Santini, D., Paterini, P., Marcu, K.B., et al. (2007). IL-6 triggers malignant features in mammospheres from human ductal breast carcinoma and normal mammary gland. J. Clin. Invest. *117*, 3988–4002.

Seki, S., Sakaguchi, H., Kitada, T., Tamori, A., Takeda, T., Kawada, N., Habu, D., Nakatani, K., Nishiguchi, S., and Shiomi, S. (2000). Outcomes of dysplastic nodules in human cirrhotic liver: a clinicopathological study. Clin. Cancer Res. *6*, 3469–3473.

Sell, S., and Leffert, H.L. (2008). Liver cancer stem cells. J. Clin. Oncol. *26*, 2800–2805.

Shin, S., Walton, G., Aoki, R., Brondell, K., Schug, J., Fox, A., Smirnova, O., Dorrell, C., Erker, L., Chu, A.S., et al. (2011). Foxl1-Cre-marked adult hepatic progenitors have clonogenic and bilineage differentiation potential. Genes Dev. *25*, 1185–1192.

Soresi, M., Giannitrapani, L., D'Antona, F., Florena, A.M., La Spada, E., Terranova, A., Cervello, M., D'Alessandro, N., and Montalto, G. (2006). Interleukin-6 and its soluble receptor in patients with liver cirrhosis and hepatocellular carcinoma. World J. Gastroenterol. *12*, 2563–2568.

Su, Y., Kanamoto, R., Miller, D.A., Ogawa, H., and Pitot, H.C. (1990). Regulation of the expression of the serine dehydratase gene in the kidney and liver of the rat. Biochem. Biophys. Res. Commun. *170*, 892–899.

Su, Q., Benner, A., Hofmann, W.J., Otto, G., Pichlmayr, R., and Bannasch, P. (1997). Human hepatic preneoplasia: phenotypes and proliferation kinetics of foci and nodules of altered hepatocytes and their relationship to liver cell dysplasia. Virchows Arch. *431*, 391–406.

Takayama, T., Makuuchi, M., Hirohashi, S., Sakamoto, M., Okazaki, N., Takayasu, K., Kosuge, T., Motoo, Y., Yamazaki, S., and Hasegawa, H. (1990). Malignant transformation of adenomatous hyperplasia to hepatocellular carcinoma. Lancet *336*, 1150–1153.

Terris, B., Cavard, C., and Perret, C. (2010). EpCAM, a new marker for cancer stem cells in hepatocellular carcinoma. J. Hepatol. *52*, 280–281.

Tsutsumi, M., Lasker, J.M., Shimizu, M., Rosman, A.S., and Lieber, C.S. (1989). The intralobular distribution of ethanol-inducible P450IIE1 in rat and human liver. Hepatology *10*, 437–446.

Verna, L., Whysner, J., and Williams, G.M. (1996). N-nitrosodiethylamine mechanistic data and risk assessment: bioactivation, DNA-adduct formation, mutagenicity, and tumor initiation. Pharmacol. Ther. *71*, 57–81.

Viswanathan, S.R., and Daley, G.Q. (2010). Lin28: A microRNA regulator with a macro role. Cell *140*, 445–449.

Wang, R., Ferrell, L.D., Faouzi, S., Maher, J.J., and Bishop, J.M. (2001). Activation of the Met receptor by cell attachment induces and sustains hepatocellular carcinomas in transgenic mice. J. Cell Biol. *153*, 1023–1034.

Weglarz, T.C., Degen, J.L., and Sandgren, E.P. (2000). Hepatocyte transplantation into diseased mouse liver. Kinetics of parenchymal repopulation and identification of the proliferative capacity of tetraploid and octaploid hepatocytes. Am. J. Pathol. *157*, 1963–1974.

Wood, L.D., Parsons, D.W., Jones, S., Lin, J., Sjöblom, T., Leary, R.J., Shen, D., Boca, S.M., Barber, T., Ptak, J., et al. (2007). The genomic landscapes of human breast and colorectal cancers. Science *318*, 1108–1113.

Yamashita, T., Forgues, M., Wang, W., Kim, J.W., Ye, Q., Jia, H., Budhu, A., Zanetti, K.A., Chen, Y., Qin, L.X., et al. (2008). EpCAM and alpha-fetoprotein expression defines novel prognostic subtypes of hepatocellular carcinoma. Cancer Res. *68*, 1451–1461.

Yang, Z.F., Ho, D.W., Ng, M.N., Lau, C.K., Yu, W.C., Ngai, P., Chu, P.W., Lam, C.T., Poon, R.T., and Fan, S.T. (2008). Significance of CD90+ cancer stem cells in human liver cancer. Cancer Cell *13*, 153–166.

Zheng, T., Wang, J., Jiang, H., and Liu, L. (2011). Hippo signaling in oval cells and hepatocarcinogenesis. Cancer Lett. *28*, 91–99.

Zhu, Z., Hao, X., Yan, M., Yao, M., Ge, C., Gu, J., and Li, J. (2010). Cancer stem/progenitor cells are highly enriched in CD133+CD44+ population in hepatocellular carcinoma. Int. J. Cancer *126*, 2067–2078.

Zöller, M. (2009). Tetraspanins: push and pull in suppressing and promoting metastasis. Nat. Rev. Cancer *9*, 40–55.

SCIENTIFIC REPORTS

Regulation of the expression of the liver cancer susceptibility gene MICA by microRNAs

Takahiro Kishikawa[1]*, Motoyuki Otsuka[1,2]*, Takeshi Yoshikawa[1], Motoko Ohno[1], Akemi Takata[1], Chikako Shibata[1], Yuji Kondo[1], Masao Akanuma[3], Haruhiko Yoshida[1] & Kazuhiko Koike[1]

[1]Department of Gastroenterology, Graduate School of Medicine, The University of Tokyo, Tokyo 113-8655, Japan, [2]Japan Science and Technology Agency, PRESTO, Kawaguchi, Saitama 332-0012, Japan, [3]Division of Gastroenterology, The Institute for Adult Diseases, Asahi Life Foundation, Tokyo 100-0005, Japan.

Hepatocellular carcinoma (HCC) is a threat to public health worldwide. We previously identified the association of a single nucleotide polymorphism (SNP) at the promoter region of the MHC class I polypeptide-related sequence A (MICA) gene with the risk of hepatitis-virus-related HCC. Because this SNP affects MICA expression levels, regulating MICA expression levels may be important in the prevention of HCC. We herein show that the microRNA (miR) 25-93-106b cluster can modulate MICA levels in HCC cells. Overexpression of the miR 25-93-106b cluster significantly suppressed MICA expression. Conversely, silencing of this miR cluster enhanced MICA expression in cells that express substantial amounts of MICA. The changes in MICA expression levels by the miR25-93-106b cluster were biologically significant in an NKG2D-binding assay and an *in vivo* cell-killing model. These data suggest that the modulation of MICA expression levels by miRNAs may be a useful method to regulate HCCs during hepatitis viral infection.

epatocellular carcinoma (HCC) is the third most common cause of cancer-related mortality worldwide[1]. Although multiple major risk factors have been identified, such as genetic factors, environmental toxins, alcohol abuse, obesity, and metabolic disorders[2], infection with hepatitis virus B (HBV) or C (HCV) remains the major etiological factor for HCC[1].

Disease progression in HBV-induced or HCV-induced HCC is a multistep phenomenon. The clinical outcomes vary among individuals[1,3,4] because disease progression is influenced by both environmental and genetic risk factors. In terms of genetic susceptibility factors for HCV-induced HCC, we previously identified a single nucleotide polymorphism (SNP) site in the 5'-flanking region of the MICA gene on 6p21.33 (rs2596452) that is strongly associated with progression from chronic hepatitis C to HCC[5]. Individuals with the risk allele A of rs2596452 showed lower serum MICA protein levels[5]. Our subsequent study revealed that the same SNP site was also significantly associated with the risk of HBV-induced HCC[6]. However, interestingly, the risk allele was G in cases of HBV infection, which differed from HCV infection, and the individuals with the risk allele showed increased MICA protein expression levels[6]. Despite the different risk alleles at the same SNP site and inverse association between serum MICA levels and HCC risks in these two etiologies, MICA protein expression levels are significantly associated with susceptibility to HCC in chronic hepatitis viral infection.

MICA is highly expressed on viral-infected and cancer cells and acts as a ligand for NKG2D to activate the antitumor effects of natural killer cells and CD8 T cells[7,8]. This NKG2D-mediated tumor rejection is considered to be effective in the early stages of tumor growth[9–11]. Thus, the expression levels of MICA on the tumor cell surface may determine the antitumor efficacy, and the levels of shedding MICA in serum may act as a decoy of NKG2D to avoid tumor rejection.

Although several stress pathways regulate the transcription of the MICA gene[12,13], cellular microRNAs are suggested to control MICA protein expression via post-transcriptional mechanisms[14,15]. Recently, nucleic-acid-mediated gene therapy has been undergoing clinical trials[16]. Therefore, to target the clinical application of our GWAS results toward prevention of chronic-hepatitis-infection-induced HCC by nucleic-acid-mediated therapy, we determined the regulatory mechanisms of MICA protein expression using miRNA overexpression and miRNA functional silencing.
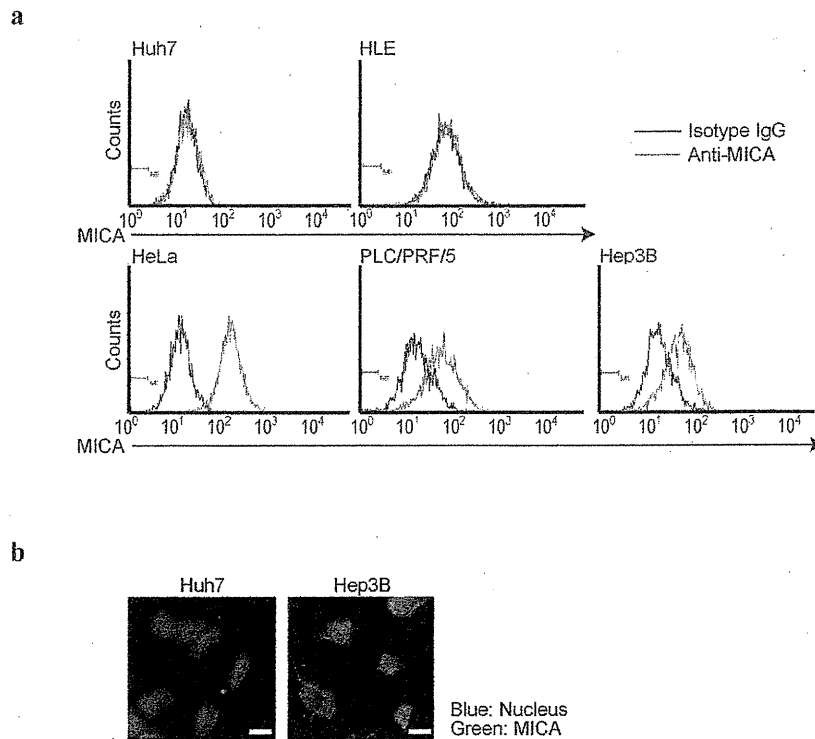
a

b

Blue: Nucleus
Green: MICA

Figure 1 | Expression of MICA protein in HCC cells. (a), Flow cytometry assessment of MICA protein expression in HCC cells (purple lines). Isotype IgG was used for background staining (black lines). HeLa cells were used as the positive control. Representative results from two independent experiments are shown. (b), Immunofluorescence staining for MICA in Huh7 and Hep3B cells. Representative images from two independent experiments are shown. Scale bar, 25 µm.

Results

HCC cell lines differentially express MICA protein. To determine MICA protein levels in HCC cells, four representative HCC cell lines (Huh7, HLE, PLC/PRF/5, and Hep3B cells) underwent flow cytometry to evaluate MICA protein expression because no appropriate antibodies against MICA protein are at present available for western blotting. HeLa cells, which are known to express MICA protein[17], were used as a positive control. Hep3B and PLC/PRF/5 cells expressed substantial MICA protein levels, Huh7 and HLE cells expressed no MICA protein (Figure 1a). This was confirmed by immunocytochemistry using Huh7 and Hep3B cells, which showed staining mainly of cell surfaces (Figure 1b). These results suggest that the MICA protein expression status depends on the cell line examined, even those from the same organ.

The MiR25-93-106b cluster regulates MICA expression. Because upregulation of MICA expression was observed in Dicer-knockdown cells[18], we hypothesized that MICA expression levels may be at least partly regulated by miRNAs. We initially tested miRNAs that might affect MICA expression using reporter constructs into which MICA 3′-untranslated region (3′UTR) sequences were cloned and by transiently overexpressing 76 mature synthetic microRNAs, which were selected on the basis of their hepatic expression level, as in our previous studies[19,20]. Among the microRNAs examined, several may target MICA 3′UTR (Supplementary Figure 1). Among them, we focused on miR93 and miR106b, which were considered to target MICA 3′UTR based partly on the results of our initial miRNA testing described above; in addition, their possible target sequences were identified in the MICA 3′UTR sequences by a computational search using TargetScan 6.0 [21]. Additional reasons that we focused on these two miRNAs were as follows: 1) these miRNAs share the same seed sequences, to which two perfect-match complementary sequences exist in the 3′UTR of MICA (Figure 2a); 2) the target

sequences are highly conserved among mammals and are thus likely to be biologically important sites; and 3) these miRNAs are located as a "miR25-93-106b cluster" on human chromosome 7q22.1, and so they may be expressed together under the same transcriptional control. We introduced mutations in the first possible miRNA target sequences of MICA 3′UTR in the reporter constructs (Supplementary Figure 2a); these sequences have a higher likelihood to be target sites, as determined by TargetScan. Co-transfection experiments revealed that reporter activity was suppressed by overexpression of a miR25-93-106b cluster-expressing plasmid (Figure 2b and Supplementary Figure 2b). The over-expression of an unrelated miR (let-7g)-expressing plasmid did not have any significant effects on the reporter activity (Supplementary Figure 2c) and the suppressive effect was lost using constructs with three point mutations in the seed sequences (Figure 2c), suggesting that miR25-93-106b directly targets these sequences and suppresses gene expression.

To confirm these effects, we generated HeLa and Hep3B cell lines that stably expressed the miR25-93-106b-cluster by transducing cells with miR25-93-106b-cluster-expressing lentiviruses (Figure 2d). As expected, the expression of the miR25-93-106b-cluster significantly suppressed MICA protein expression (Figure 2e). However, the expression levels of endogenous miR93 and 106b were not always proportional to the levels of MICA protein expression in the cell lines examined (Supplementary Figure 3). These results suggest that MICA protein expression can be regulated by miR93 and 106b, but that its expression is simultaneously endogenously regulated by other factors (possibly by promoter activities, including epigenetic changes).

Inhibition of miR25-93-106b function increases MICA protein expression. To develop methods of enhancing MICA protein expression levels based on the above results, we examined the

2

a

MICA 3' UTR

5'.....ATTTCAGCCTCTGATGTCAGCTCTTGGGTCCACTGGCTCCACTGAGGGCACCTAGACTCTACAGCC
AGGCGGCTGGAATTGAATTCCCTGCCTGGATCTCACAAGCACTTTCCCTCTTGGTGCCTCAGTTTCCTGA
CCTATGAAACAGAGAAAATAAAAGCACTTATTTATTGTTGTTGGAGGCTGCAAAATGTTAGTAGATATGA
GGCATTTGCAGCTGTGCCATATTAATTGGTGTCATTGTTTTTGTTGTTTTCGTATTATTATTTTTTTTTTTTA
AGACAGAGTCTCAGGCCA 3'

5'.....CTGCCTGGATCTCACAAGCACTTT.....3'
     |:|:|||| | | |! |||||||!|
     GAUGGACG U GCUUG UCGUGAAAC miR-93

5'.....CTGCCTGGATCTCACAAGCACTTT.....3'
     :|: || | ||||||||
     UAGACGUGACAG UCGUGAAAU miR-106b
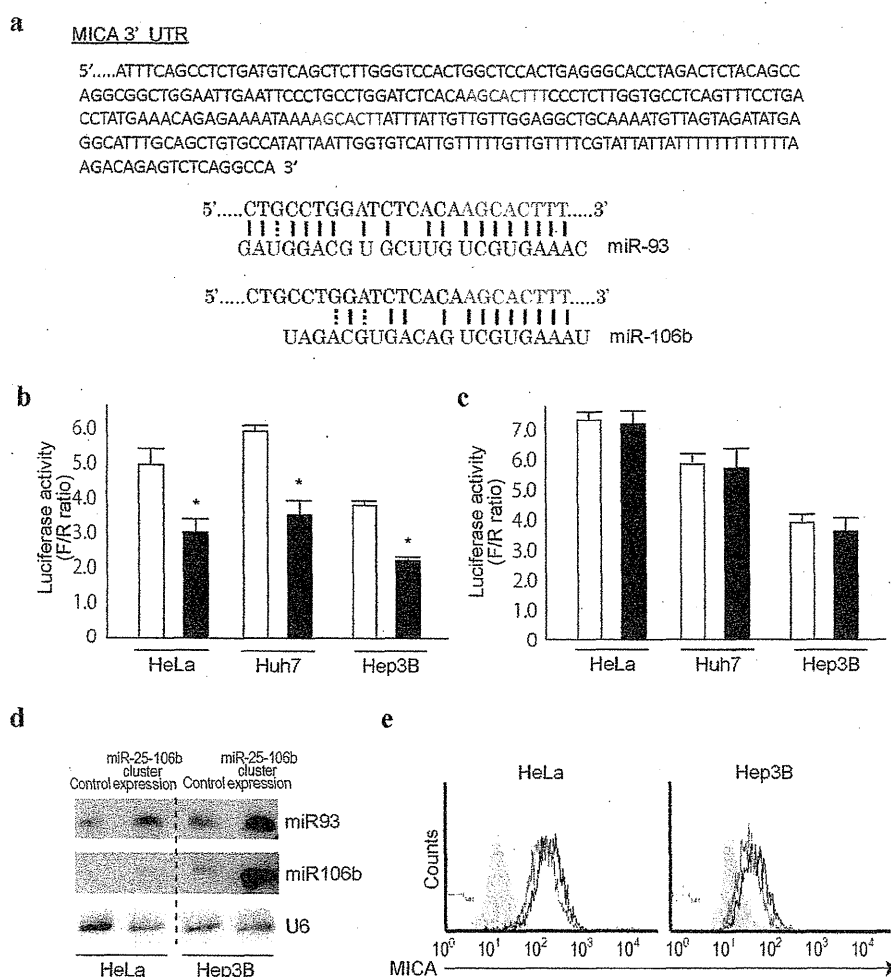
b

c

d

e

Figure 2 | miR93 and 106b target MICA 3'UTR. (a), Sequences of MICA 3'UTR (upper). Letters in red are the sequences completely matched with the seed regions of miR93 and 106b. The complementarities between the first predicted target in the MICA 3'UTR and miRNA sequences are shown below. (b), (c), Cells were co-transfected with pGL4-TK (renilla luciferase as an internal control), Luc-MICA-3'UTRwt (b) or Luc-MICA-3'UTRmut (c), and either an empty control vector (white bar) or miR25-93-106b-cluster expression plasmid (black bar). Data shows the means ± s.d. of the raw ratios (F/R) obtained by dividing firefly luciferase values with renilla luciferase values of three independent experiments. *p < 0.05. (d), miR93 and miR106b expression levels in control and stably miR25-93-106b cluster-expressing cells were determined by northern blotting. U6 levels were used as a loading control. Representative images from two independent experiments are shown. Full-length blot images are available in Supplementary Figure 5. (e), Suppression of MICA expression by overexpression of miRNA93 and 106b. Flow cytometry assessment of MICA protein expression in control (black lines) and stably miR25-93-106b cluster-expressing HeLa and Hep3B cells (red lines). Gray-shaded histograms represent the background staining using isotype IgG. Representative results from two independent experiments are shown.

effects of functional downregulation of miR25-93-106b on MICA expression. We first performed a reporter assay of transient functional silencing of miR25-93-106b using a construct that produces mature anti-sense RNAs designed to silence miR25-93-106b function. As expected, the reporter activities with MICA 3'UTR sequences were enhanced by the functional silencing of miR25-93-106b in HeLa, Hep3B, and Huh7 cells (Figure 3a). However, such effects were not observed using mutant reporter constructs not targeted by those miRNAs (Figure 3b), suggesting that the enhancing effects of the reporter activities were miRNA-dependent.

Next, HeLa, Hep3B, and Huh7 cells were stably transduced with a lentivirus that expresses anti-sense RNAs as described above, and MICA protein expression levels were determined by flow cytometry. Consistent with the reporter assay results, MICA protein expression was increased in HeLa and Hep3B cells by the functional silencing of miR25-93-106b (Figure 3c). However, in Huh7 cells, which express no MICA protein in the normal state, silencing of miR25-93-106b had no effect on MICA protein expression (Figure 3c). These results

suggest that MICA protein expression levels can be regulated by modulating miRNA function, albeit only if at least a small quantity of MICA protein is present. In contrast, modulation of miRNA function does not influence MICA protein expression levels when the MICA protein is not expressed, but this could be because there are other forms of regulation at extremely low levels.

MICA protein levels are related to tumor susceptibility to NK cells. To determine the consequences of the modulation of MICA protein expression levels by miRNAs, we first determined the binding ability of NKG2D, a receptor of MICA, using HeLa and Hep3B cells overexpressing the miR25-93-106b cluster or with silencing of miR25-93-106b function. As expected, the levels of NKG2D binding to the cells, theoretically through binding to MICA, were decreased in HeLa and Hep3B cells overexpressing the miR25-93-106b cluster (Figure 4a). On the contrary, the levels of NKG2D binding to the cells were increased in HeLa and Hep3B cells in which miR25-93-106b function had been silenced (Figure 4b).